The study of the excited states of ^{26}Mg below 11 MeV by inelastic electron scattering

1974 J. Phys. A: Math. Nucl. Gen. 7 936

(http://iopscience.iop.org/0301-0015/7/8/005)

J. Phys. A: Math., Nucl. Gen., Vol. 7, No. 8, 1974. Printed in Great Britain.

The study of the excited states of ^{26}Mg below 11 MeV by inelastic electron scattering

E W Lees, A Johnston, S W Brain, C S Curran†, W A Gillespie and R P Singhal

Kelvin Laboratory, University of Glasgow, Glasgow, UK

Received 20 December 1973

Abstract. The excited states of ^{26}Mg below 11 MeV excitation energy were studied by inelastic electron scattering in the momentum transfer range 0·4 to 1·05 fm^{-1}. At lower excitation energies, several spin–parity uncertainties were resolved and the spin–parity assignments were extended up to 11 MeV. Ground state reduced transition probabilities and transition radii were measured for 29 levels. The reduced transition probabilities were found to be more accurate than existing experimental results. The form factors and transition probabilities are compared to various theoretical predictions.

1. Introduction

The nucleus ^{26}Mg is one of the least studied even–even 2s–1d shell nuclei from both an experimental and theoretical standpoint. The published level spectrum of Endt and Van der Leun (1967) contained several levels of unknown spin and parity for excitation energies as low as 4·3 MeV. Since then, the spin–parity assignments have been extended up to 7 MeV excitation energy and several of these (Häusser *et al* 1968, Canada *et al* 1969, Blair and Naqib 1970) were in disagreement with those of Endt and Van der Leun (1967). Only the 180° inelastic electron scattering experiment of Bendel *et al* (1968) has identified spins and parities for states between 7 and 11 MeV excitation energy. However, their experiment was primarily sensitive only to magnetic transitions and, in contrast, an inelastic electron scattering experiment performed at conventional angles should excite a greater variety of levels.

The lifetimes of states up to an excitation energy of 6 MeV have been measured by Häusser *et al* (1968) and Durell *et al* (1972). The results of these two experiments are in good agreement for most levels. However, since both experiments employed the Doppler shift attenuation (DSA) method of lifetime measurement, it is of interest to compare their results with an independent experimental technique.

There have been three previous electron scattering experiments performed on ^{26}Mg. The earliest of these (Titze and Spamer 1966) studied the excitation region from 7 to 14 MeV and determined the electromagnetic character of the states. Neither reduced transition probabilities nor transition radii were determined. The experiment of Bendel *et al* (1968) studied the excitation region from 8·5 to 14 MeV at a scattering angle of 180° and a maximum incident electron energy of 55 MeV. However, their angle of scatter and energy range necessarily restricted them to observing M1 and M2 transitions.

† Now at University College, University of London.

The third electron scattering experiment (Khvastunov *et al* 1970) studied only the first excited state at 1·809 MeV but the experimental resolution ($\simeq 2$ MeV) was too poor for this state to be clearly resolved from the elastic peak. An improvement on this resolution is obviously desirable.

Since the ground state of ^{26}Mg is 0^+, by identifying the properties of a transition excited in an electron scattering experiment, the spin and parity of the inelastic level can be uniquely assigned and the reduced transition probability and transition radius can thus be determined. Furthermore, in the momentum transfer range available at the Kelvin Laboratory, certain states are preferentially excited and this partially alleviates the problem of high level density. In addition, in contrast with other electromagnetic probability measurement, the electron scattering technique affords a unique test of theoretical nuclear models since one also measures the radial dependence of the transition matrix element.

Thus, the present work was undertaken to measure the spins, parities, ground state reduced transition probabilities and transition radii of the excited states of ^{26}Mg below 11 MeV excitation energy and to use the experimentally determined form factors as a test of nuclear models for ^{26}Mg.

In § 2, a brief statement of the theoretical formalism is given. Sections 3, 4 and 5 describe the experimental details and data analysis procedures. The experimental results are listed in § 6 and compared to other existing measurements. The final sections discuss the model dependence of the electron scattering results and the theoretical comparisons.

2. Summary of electron scattering formalism

The theoretical formalism employed in the analysis of the experimental data is detailed in Johnston and Drake (1974). However, the most important features are reproduced below.

In PWBA, the experimental cross section can be written as (De Forest and Walecka 1966)

$$\left(\frac{d\sigma}{d\Omega}\right)_{exp} = \sigma_M \eta F^2(q, \theta),$$

where σ_M is the Mott cross section, η is the nuclear recoil factor and $F^2(q, \theta)$ is the nuclear form factor.

For momentum transfers greater than 0·3 fm^{-1}, the form factor can be expanded as

$$F^2(q, \theta) = F_C^2(q) + [\tfrac{1}{2} + \tan^2(\tfrac{1}{2}\theta)](F_e^2(q) + F_m^2(q)) \quad (1)$$

which allows separation of the transverse and longitudinal (or Coulomb (F_C)) form factors by an angular dependence study. The transverse electric (F_e) and transverse magnetic (F_m) form factors are of opposite parity. The dependence of the form factor on momentum transfer allows a determination of the multipolarity of the transition and the longitudinal–transverse separation determines the parity. Thus, for nuclei with 0^+ ground states, the spin and parity of the excited states are uniquely determined.

To extract spectroscopic parameters from inelastic electron scattering form factors obtained at values of intermediate momentum transfer, one uses various phenomenological nuclear models. In the present experiment, the Tassie hydrodynamical model (Tassie 1956) and the generalized Helm model (Rosen *et al* 1967) were employed, both of

which have been discussed in Johnston and Drake (1974). The extracted spectroscopic parameters are the ground state reduced transition probabilities and the transition radii for the various excited states. The former parameter is related to the nuclear form factor by

$$B(\mathrm{E}L, \uparrow) = \frac{Z^2}{4\pi} \frac{[(2L+1)!!]^2}{\omega^{2L}} F^2_{\mathrm{C},L}(q = \omega)$$

$$B(\mathrm{M}L, \uparrow) = \frac{Z^2}{4\pi} \left(\frac{L}{L+1} \right) \frac{[(2L+1)!!]^2}{\omega^{2L}} F^2_{\mathrm{m},L}(q = \omega)$$

where $B(^{\mathrm{E}}_{\mathrm{M}}L, \uparrow)$ is the reduced electric/magnetic transition probability from the ground state to the excited state for the transition of multipolarity L. In the present work, the definitions of Rosen *et al* (1967) were used for the transition radii.

A DWBA phase shift code (Tuan *et al* 1968) is used in the analysis of the data to include the distortion of the incoming and outgoing electron waves in the Coulomb field of the nucleus. For light nuclei, the Coulomb distortion is small (Schucan 1968, Drechsel 1968) and a correction factor f_c can be introduced to account for the difference between the PWBA and the DWBA cross sections, that is,

$$f_c = \frac{(\mathrm{d}\sigma/\mathrm{d}\Omega)_{\mathrm{DWBA}}}{(\mathrm{d}\sigma/\mathrm{d}\Omega)_{\mathrm{PWBA}}}. \tag{2}$$

These correction factors may be used to convert the experimentally determined cross sections $(\mathrm{d}\sigma/\mathrm{d}\Omega)_{\mathrm{exp}}$ into equivalent PWBA values $f_c^{-1}(\mathrm{d}\sigma/\mathrm{d}\Omega)_{\mathrm{exp}}$ so that analysis can proceed in PWBA. As will be discussed in § 4, the use of correction factors considerably reduces the amount of computing time required for analysis of the electron scattering form factors. The equivalent PWBA data can also be directly compared with theoretical predictions.

For the electron energies and scattering angles used in this experiment, the correction factors for a given level are solely dependent on the momentum transfer to an accuracy of 4%. Theissen (1972) has shown that the correction factors are fairly insensitive to variations in the transition radii and the excitation energy and are almost independent of the nuclear model describing the excitation.

3. Experimental details

The 120 MeV electron scattering facility described by Hogg *et al* (1972) was used to study the excited states of ^{26}Mg in the momentum transfer range 0·4 to 1·05 fm^{-1} for the first excited state and in the range 0·5 to 1·05 fm^{-1} for all other levels below 11 MeV excitation energy. The incident energies and scattering angles used to study the first excited state are shown in table 1. Table 2 lists these values for the remaining excited states. A longitudinal transverse separation of the cross section was performed at three scattering angles and at a constant momentum transfer of 0·8 fm^{-1}, since all the multipolarities excited in this experiment are observed quite clearly at this value of momentum transfer.

The target used was a self-supporting metal foil of thickness 46·8 mg cm^{-2} and enriched to 99·7% in ^{26}Mg. The maximum analysed current was 5 μA and the counting rate was limited to one back detector pulse per two beam pulses to eliminate counting losses. The data were obtained in a similar manner to that described elsewhere (Johnston and Drake 1974). In all cases the inelastic spectra were measured relative to the elastic

Table 1. Experimental details for the 1·809 MeV level.

Run	E_i (MeV)	θ (deg)	q_{IN} (fm^{-1})	A_{IN}/A_{EL} ($\times 10^{-2}$)	Error (%)
1	72·75	65	0·39	0·31	9·9
2	60·01	120	0·52	1·13	6·5
3	82·04	120	0·71	4·82	4·2
4	92·15	120	0·80	9·68	4·6
5	104·31	120	0·90	21·3	5·5
6	110·71	120	0·96	33·8	5·0
7	114·37	120	0·99	43·1	5·8
8	110·45	140	1·04	64·4	5·7

Table 2. Electron energies and angles employed in the present experiment.

Run	E_i (MeV)	θ (deg)	q_{EL} (fm^{-1})
1	95·74	120	0·84
2	110·71	120	0·97
3	82·75	120	0·73
4	85·09	90	0·61
5	110·45	140	1·05
6	56·89	120	0·50
7	91·28	120	0·80
8	84·16	140	0·80
9	81·36	153	0·80

scattering. Typical resolution was 0·15% of the incident energy. The background counting rate of 0·6 counts/mC was negligible.

A typical inelastic spectrum is shown in figures 1(*a*) and (*b*). The spectrum above 6 MeV is complex but one can extract the inelastic cross sections by lineshape analysis as will be discussed in § 4.

4. Data analysis

4.1. Extraction of form factors

The form factor for an inelastic level can be obtained from the inelastic peak areas since

$$F^2_{IN}(q, \theta) = \frac{A_{IN}}{A_{EL}} R_c F^2_{EL}(q, \theta) \tag{3}$$

where A_{IN}/A_{EL} is the inelastic to elastic peak area ratio, R_c is the ratio of the inelastic to elastic radiative, bremsstrahlung and ionization corrections and F^2_{EL} is the elastic form factor. The present experimental objective is therefore to extract for each run the area ratios of the inelastic peaks with respect to the elastic peak.

The experimental data were first corrected for the efficiencies, spacings and detector bites of the individual detectors (Hogg *et al* 1972). For each run, the elastic peak shape was fitted with a linear combination of polynomials and gaussians (Johnston and Drake

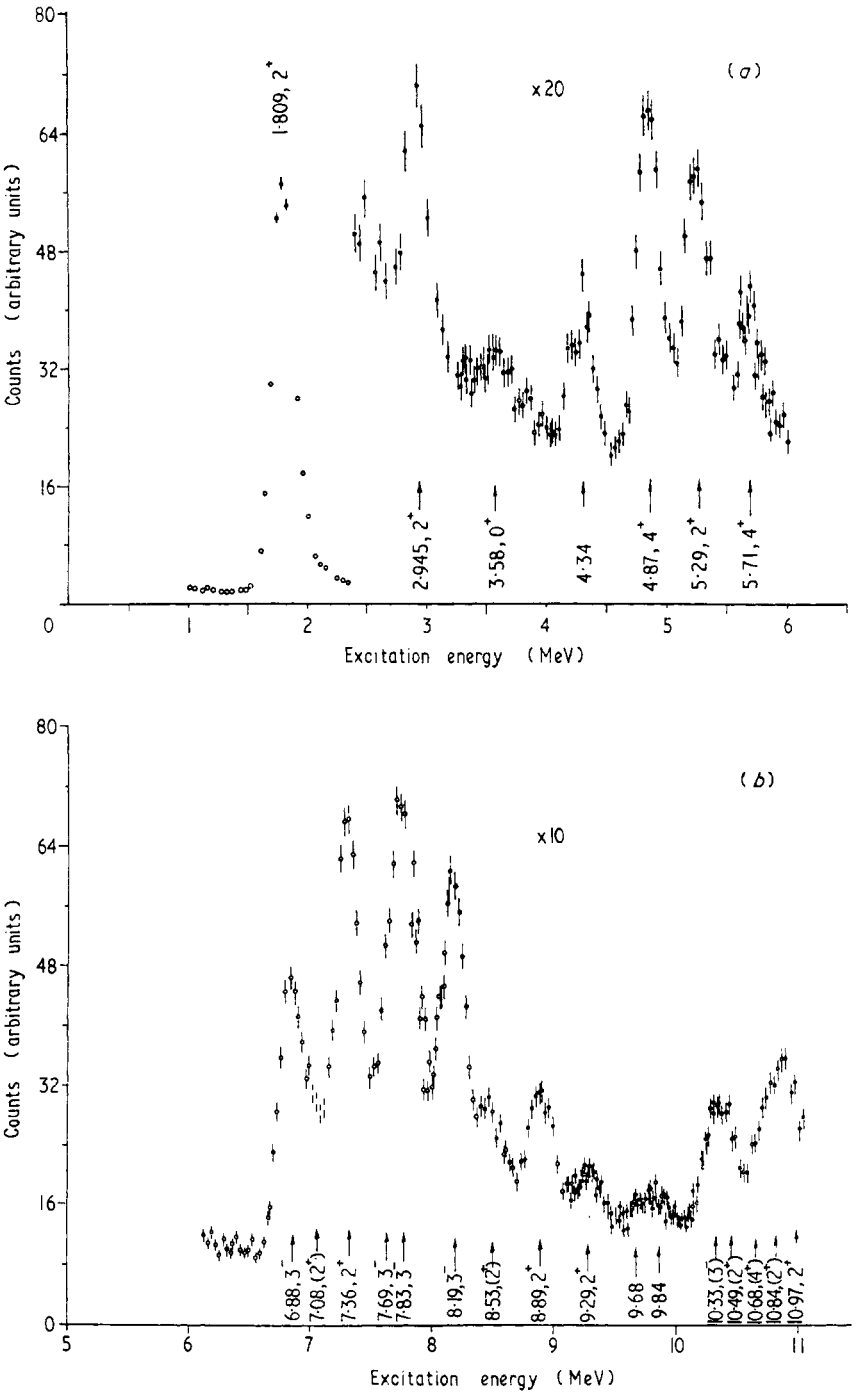

Figure 1. (*a*) Spectrum of inelastically scattered electrons from ^{26}Mg for the excitation energy range up to 6 MeV. The arrows indicate the measured excitation energies (in MeV) and the deduced spin and parity assignments. The elastic peak has a height of 90 units of the ordinate scale. (*b*) Same as for (*a*) except that the excitation range is 6 to 11 MeV. For both parts E_i = 110·45 MeV, θ = 140°.

1974). The inelastic spectrum was then fitted by using the elastic peak shape and allowing the excitation energy and the height of each inelastic level to be free parameters. In addition, the three elastic radiation tail parameters were allowed to vary in the fitting process to incorporate the effects of instrumental rescattering (Duguay *et al* 1967) which produces a smooth background of a shape similar to the elastic radiation tail (Lees 1972, Johnston and Drake 1974). Thus at any point with excitation energy E_x, the fitted function for m inelastic levels is given by

$$F(E_x) = A + \frac{B}{E_x} + \frac{C}{E_x^2} + \sum_{i=1}^{m} h_i f\left((E_x - E_x^i)\frac{R_{EL}}{R_{IN}}\right)$$

where h_i is the relative height of the inelastic to the elastic peak, $f(E_x^i)$ is the elastic peak shape, $(E_x - E_x^i)$ takes into account the excitation energy E_x^i of the ith inelastic peak and R_{EL}/R_{IN} allows for the constant dispersion of the magnetic spectrometer which results in a slight improvement in the inelastic peak resolution as the excitation energy increases.

Occasionally, fits with a poor χ^2 resulted from insufficient levels being included in the excitation region. In this manner, it was discovered that two levels were consistently required to fit the 7·8 MeV region and three levels for the 10·6 to 10·9 MeV region. An example of this is shown in figures 2(*a*) and (*b*). Good agreement was obtained for the excitation energies evaluated by the program from different runs (table 3). The excitation energies measured by the present experiment are compared to values deduced from other studies in table 4.

Table 5 lists the measured ratios of inelastic to elastic peak areas for all transitions except the 1·809 MeV level which are listed in table 1. Before the inelastic form factors can be deduced from these area ratios, it is necessary to evaluate R_c of equation (3).

We used the Schwinger radiative correction extended by Maximon (1969) for inelastic scattering. The correction factors as given by Bergstrom *et al* (1971) and Isabelle and Bishop (1963) were used for the ionization and bremsstrahlung corrections respectively. The differences between the total elastic and inelastic corrections even for levels of high

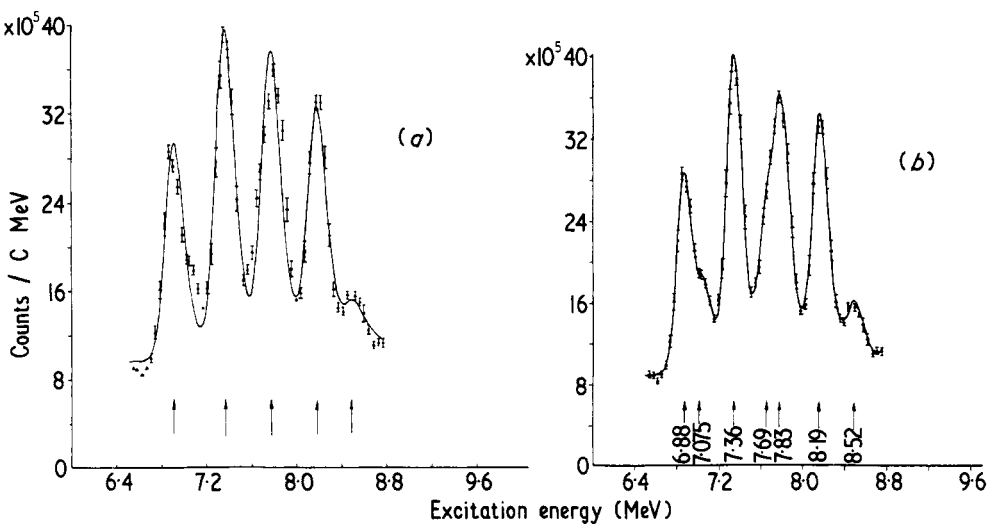

Figure 2. (*a*) Shows the resulting fit to the data when only the excitations of 5 levels are assumed. (*b*) Shows the resulting fit upon the inclusion of a further 2 levels. The arrows indicate the fitted excitation energies (in MeV). For both parts $E_i = 110{\cdot}8$ MeV, $\theta = 120°$.

Table 3. Measured excitation energies of the doublet at 7·75 MeV.

Run	Measured excitation energies of the doublet (MeV)	
1	7·705	7·834
2	7·655	7·794
3	7·679	7·816
4	7·705	7·891
5	7·661	7·817
6	7·736	7·837
7	7·688	7·824
8	7·664	7·812
9	7·729	7·840
Mean	7·691	7·830
Error in mean	±0·0104	±0·0096
+0·1 % Rawson error	0·00769	0·00783
Final results	7·691 ± 0·018	7·830 ± 0·017

Table 4. Excitation energies, spins and parities deduced from the present experiment compared to the values deduced from previous measurements. Spins and parities given in parenthesis denote tentative values. Uncertainties in excitation energy of less than 1 keV have not been shown. The previous measurements are those discussed in § 6.

Previous measurements		Present measurements		Previous measurements		Present measurements	
$E_x(\pm\Delta E_x)$ MeV (±keV)	J^π	$E_x(\pm\Delta E_x)$ MeV (±keV)	J^π	$E_x(\pm\Delta E_x)$ MeV (±keV)	J^π	$E_x(\pm\Delta E_x)$ MeV (±keV)	J^π
1·809	2^+	1·809 (5)	2^+	7·358 (10)	—	7·364 (15)	2^+
2·938	2^+	2·945 (10)	2^+	—	—	7·691 (18)	3^-
3.588	0^+	3.579 (11)	0^+	—	—	7·830 (17)	3^-
3·942	3^+	—	—	8·185 (2)	—	8·181 (16)	3^-
4·320 (1)	4^+	—	—	8·215 (15)	(1^+)	8·22	(1^+)
4·332	$(1, 2)^+$	4·337 (25)	2^+	8·521 (10)	1^+	8·526 (19)	(2^+)
4·350	3^+	—	—	8·902 (2)	—	8·892 (14)	2^+
4·835 (1)	2^+	—	—	9·246 (4)	1^+	9·25	(1^+)
4·901 (1)	4^+	4·875 (15)	4^+	9·295 (12)	—	9·287 (19)	2^+
4·972 (1)	0^+	4·979 (16)	0^+	9·707 (15)	—	9·727 (25)	—
5·291 (1)	$(0, 1, 2)^+$	5·294 (19)	2^+	9·814 (15)	1^+	9·80	(1^+)
5·474 (1)	4^+	5.449 (50)	4^+	9·841 (15)	—	9·860 (18)	2^+
5·690 (1)	$(1, 2)^+$	—	—	10·18 (30)	1^+	10·199 (27)	1^+
5·715 (1)	$(3, 4)^+$	5·720 (22)	4^+	10·316 (15)	—	10·330 (20)	(3^-)
6·126 (1)	(2^+)	—	—	10·358 (15)	—	—	—
6·256 (3)	0^+	6·216 (20)	(0^+)	10·483 (15)	—	10·491 (23)	2^+
6·616 (10)	(3^+)	—	—	10·63 (30)	1^+	10·65 (50)	1^+
6·742 (3)	$(2, 3)^+$	—	—	—	—	10·680 (34)	4^+
6·878 (1)	3^-	6·876 (14)	3^-	—	—	10·838 (24)	2^+
7·059 (2)	(1^-)	—	—	10·98	—	10·990 (27)	2^+
7·097 (2)	(2^+)	7·082 (16)	2^+	11·00	—	—	—

excitation energy, are less than 1 % at all momentum transfers measured. These differences are negligible compared to the uncertainties which arise in the measurement of the inelastic form factors at higher excitation energies (see § 5).

Table 5. Area ratios for the transitions observed in the present experiment. The exponent follows the symbol E and the figures in parenthesis are the percentage errors in the square of the inelastic form factor.

Run / E_x (MeV)	1	2	3	4	5	6	7	8	9
2·945	3·32E – 3(5·4)	1·04E – 2(6·8)	1·77E – 3(15·7)	5·77E – 4(15·5)	2·06E – 2(11·5)	2·50E – 4(20·7)	2·46E – 3(11·2)	2·20E – 3(9·2)	2·93E – 3(8·2)
3·579	1·15E – 3(8·4)	2·35E – 3(16·0)	7·66E – 4(11·0)	3·54E – 4(9·1)	4·30E – 3(21·3)	2·16E – 4(21·0)	1·25E – 3(15·9)	9·71E – 4(8·0)	1·23E – 3(16·3)
4·337	1·32E – 3(6·8)	3·50E – 3(9·7)	6·10E – 4(7·5)	1·46E – 4(30·0)	9·80E – 3(16·0)		9·70E – 4(25·0)		9·04E – 4(16·3)
4·875	1·47E – 3(15·7)	7·94E – 3(7·5)	3·48E – 4(12·8)		2·70E – 2(9·7)		1·13E – 3(14·9)	1·00E – 3(15·9)	1·22E – 3(21·0)
4·979	6·66E – 4(25·0)		4·20E – 4(15·7)	2·01E – 4(21·2)		1·12E – 4(50·0)	5·87E – 4(23·5)	9·02E – 4(17·8)	9·60E – 4(21·0)
5·294	2·05E – 3(15·7)	8·15E – 3(7·5)	9·25E – 4(6·7)	3·66E – 4(10·8)	2·00E – 2(11·4)	1·16E – 4(16·0)	1·74E – 3(7·2)	1·76E – 3(11·3)	2·15E – 3(11·9)
5·449	2·33E – 4(35·0)	5·26E – 4(50·0)			4·90E – 3(40·0)				
5·720	6·00E – 4(15·7)	2·71E – 3(11·4)	1·63E – 4(20·0)		9·42E – 3(11·4)		4·22E – 4(11·8)	2·18E – 4(100.0)	3·80E – 4(50·0)
6·216	3·40E – 4(20·0)		1·81E – 4(40·0)			7·17E – 5(60·0)	1·62E – 4(40·0)	3·05E – 4(50·0)	
6·876	4·01E – 3(6·7)	1·60E – 2(7·1)	1·27E – 3(6·6)	4·34E – 4(10·9)	4·10E – 2(8·4)	1·18E – 4(25·0)	2·55E – 3(7·0)	2·82E – 3(9·3)	2·70E – 3(11·5)
7·082	1·74E – 3(11·0)	5·13E – 3(9·6)	7·58E – 4(6·9)	3·15E – 4(15·5)	1·59E – 2(16·1)	1·20E – 4(25·0)	1·24E – 3(11·2)	1·48E – 3(11·2)	1·63E – 3(16·3)
7·364	7·45E – 3(5·9)	2·44E – 2(5·7)	2·90E – 3(5·8)	9·79E – 4(6·1)	6·39E – 2(7·4)	2·97E – 4(30·0)	5·34E – 3(7·7)	6·19E – 3(9·2)	7·10E – 3(7·5)
7·691	2·27E – 3(11·0)	1·12E – 2(7·8)	8·50E – 4(8·3)	3·79E – 4(15·5)	3·74E – 2(16·0)	9·02E – 5(25·0)	2·07E – 3(9·5)	1·63E – 3(18·0)	2·18E – 3(9·5)
7·830	4·21E – 3(9·3)	1·73E – 2(8·0)	1·26E – 3(8·3)	2·91E – 4(15·0)	4·73E – 2(13·2)	8·88E – 5(25·0)	2·84E – 3(9·5)	3·64E – 3(15·7)	3·64E – 3(10·0)
8·181	5·10E – 3(5·6)	1·87E – 2(9·5)	1·75E – 3(5·3)	6·58E – 4(10·6)	4·39E – 2(11·4)	1·60E – 4(15·0)	3·43E – 3(6·9)	3·50E – 3(11·3)	4·66E – 3(7·4)
8·526	1·04E – 3(10·3)	3·98E – 3(20·0)	3·87E – 4(11·0)	5·66E – 5(40·0)	9·47E – 3(16·3)	5·15E – 5(100.0)	7·02E – 4(20·0)	1·04E – 3(13·6)	2·03E – 3(10·3)
8·892	2·28E – 3(7·0)	8·04E – 3(7·5)	9·92E – 4(9·2)	4·07E – 4(10·8)	1·70E – 2(9·8)	2·08E – 4(15·0)	1·67E – 3(11·2)	1·93E – 3(9·6)	1·87E – 3(9·3)
9·287	7·24E – 4(13·9)	2·18E – 3(20·0)	5·16E – 4(11·0)	1·98E – 4(15·0)	5·70E – 3(13·5)	1·42E – 4(20·0)	7·66E – 4(11·2)	6·07E – 4(20·0)	8·44E – 4(16·2)
9·727	2·94E – 4(21·0)	4·22E – 4(50·0)	8·78E – 5(50·0)	5·04E – 5(50·0)	2·46E – 3(60·0)	7·22E – 5(70·0)	2·80E – 4(25·0)		1·57E – 3(30·0)
9·860	7·36E – 4(16·0)	2·29E – 3(25·0)	2·94E – 4(20·0)	1·31E – 4(20·0)	3·92E – 3(40·0)	8·30E – 5(50·0)	4·52E – 4(15·9)	6·05E – 4(16·0)	1·39E – 3(11·8)
10·199	4·49E – 4(50·0)	2·13E – 4(50·0)	2·07E – 4(30·0)	1·33E – 4(40·0)		1·96E – 4(25·0)	1·97E – 4(50·0)	4·32E – 4(20·0)	1·05E – 3(15·0)
10·330	1·54E – 3(13·1)	5·53E – 3(16·0)	5·05E – 4(15·7)		1·35E – 2(20·0)	1·50E – 4(30·0)	8·19E – 4(13·0)	9·05E – 4(20·0)	1·25E – 3(11·8)
10·491	1·16E – 3(11·3)	3·92E – 3(16·0)	4·22E – 4(15·5)		1·22E – 2(20·0)	1·08E – 4(50·0)	9·00E – 4(11·2)	1·25E – 3(25·0)	1·41E – 3(16·2)
10·669	4·72E – 4(25·0)	2·60E – 3(40·0)	2·69E – 4(25·0)		1·27E – 2(40·0)	1·82E – 4(50·0)	4·22E – 4(25·0)	8·61E – 4(30·0)	1·31E – 3(21·0)
10·838	2·29E – 3(11·3)	5·60E – 3(25·0)	8·74E – 4(20·0)		1·87E – 2(30·0)		1·49E – 3(11·4)	1·69E – 3(25·0)	1·90E – 3(16·2)
10·990	2·04E – 3(13·0)	6·25E – 3(16·0)			1·40E – 2(30·0)		1·44E – 3(11·4)	1·35E – 3(16·0)	1·65E – 3(16·2)

The value of the elastic form factor was evaluated for each experimental run from the ground state charge parameters given in § 6 using the phase shift code of Rawitscher and Fischer (1961). The inelastic form factors were obtained using equation (3) and are defined with respect to the Mott cross section. The longitudinal–transverse separations of the form factors were then obtained and several examples of these are shown in figures 3(*a*) and (*b*).

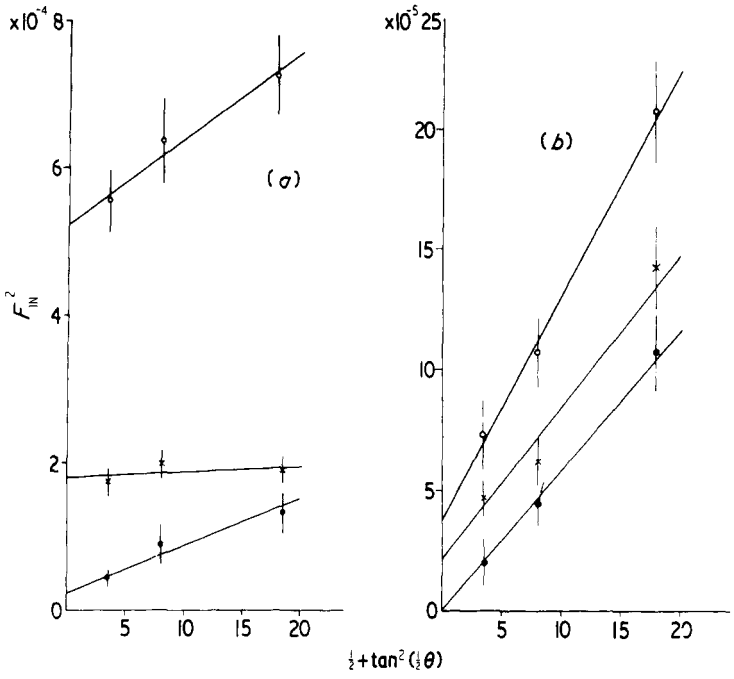

Figure 3. The longitudinal–transverse separation of the inelastic form factors. Examples shown are: in (*a*) ○ 7·364 MeV, × 8·892 MeV and ● 10·669 MeV; in (*b*) ○ 8·526 MeV, × 9·860 MeV and ● 10·199 MeV.

4.2. Fitting procedure for phenomenological models

4.2.1. Tassie model. The DWBA program DUELS of Tuan *et al* (1968) with the transition charge density of Tassie (1956) and the two-parameter Fermi model for the ground state charge distributions was used to fit the form factors of the most prominent states, namely,

$$\rho_{\mathrm{tr}}^{L}(r) = N_L r^{L-1} \frac{\mathrm{d}\rho_0(r)}{\mathrm{d}r}$$

$$\rho_0(r) = \rho_{\mathrm{N}}\left[1+\exp\left(\frac{(r-c)}{t/4{\cdot}4}\right)\right]^{-1}$$

where the symbols have their usual meaning. As is customary, c and t were allowed to vary in the fitting procedure to define an inelastic transition charge density. (To avoid confusion, the elastic charge distribution parameters will be denoted by c and t whilst the inelastic transition distribution parameters will be denoted by c_{tr} and t_{tr}). The experimental form factors were fitted by minimizing the χ^2 function using the computer code VA05A of Powell (1971).

It was found that for the present momentum transfer range, experiments performed on the lighter nuclei are sensitive to the transition radius R_{tr} rather than the individual parameters c_{tr} and t_{tr} (Johnston and Drake 1974). For the weaker or poorly defined transitions, t_{tr} was arbitrarily fixed at the value obtained for the elastic skin thickness and only c_{tr} was varied. To minimize the computing time, correction factors were used to convert the data into equivalent PWBA data as discussed in § 2. Analysis of the equivalent PWBA data was on average a factor of 15 faster. Self-consistent checks on the DWBA and equivalent PWBA fits gave better than 1 % agreement.

4.2.2. Generalized Helm model. In its present form, the Tassie model is incapable of analysing monopole transitions and electric transitions with transverse strengths in excess of that calculated from the continuity equation (Siegert theorem) (Rosen *et al* 1967). However, the generalized Helm model of Rosen *et al* (1967) is capable of phenomenologically analysing all electromagnetic transitions. In addition, analysis of the data using a different phenomenological model should yield a useful indication of the model dependence of the deduced spectroscopic parameters, ie the extent to which the results are restricted by the assumed form of a nuclear model.

Equivalent PWBA form factors were fitted by allowing the radius parameter and the strength parameters to vary. The surface thickness parameter was held fixed at $g = 1{\cdot}062$ fm since this was the value obtained from a fit of the elastic scattering form factor. Following Rosen *et al* (1967), the radius parameter $\bar{R}$ was fixed at the value $1{\cdot}25\,A^{1/3}$ for magnetic transitions and the two strength parameters γ^+ and γ^- were varied to fit the data.

5. Error estimation and treatment

The main sources of error are listed in table 6. It will be noticed that the main source of error arises from the quality of the inelastic fit to the experimental data. Where the levels are both small and densely populated, any small uncertainty in the fitting of the underlying tail summation of elastic and lower lying inelastic levels can cause substantial errors in the deduced area ratios. For example, in figure 2(*b*) the error was 3 % for the 7·364 MeV level and 15 % for the 8·526 MeV level. The total error in the square of the inelastic form factor was obtained by adding the individual components in quadrature and it is this error which is given in tables 1 and 5.

Table 6. Summary of the possible sources of error arising in the present experiment.

Source of error	Magnitude (%)
Stability and reproducibility	$\leqslant \pm 1{\cdot}5$
SEM stability	$\pm 0{\cdot}5$
Detector efficiencies	$\pm 2{\cdot}2$
Counting statistics	$\leqslant \pm 5$
Angular acceptance of spectrometer	$\leqslant \pm 0{\cdot}4$
Error in setting spectrometer angle	$\leqslant \pm 0{\cdot}4$
Error in the elastic form factor	$\leqslant \pm 3{\cdot}5$
Quality of inelastic fit	$\pm 1{\cdot}5 \rightarrow 50$
Counting losses	$\ll -2{\cdot}5$

To estimate the errors in the fitted model parameters, the criterion of Cline and Lesser (1970) was used. χ^2 parabolas were constructed for each parameter whilst the remaining parameters were varied in order to obtain a true estimate of the error.

For the generalized Helm model, a closed analytic expression exists for the matrix element and the error calculation is easily performed. These errors are listed in table 7. No error has been quoted for the parameter β of the generalized Helm model since it is coupled to the errors in $B(\mathrm{E2}, \uparrow)$ and R.

Since the transition matrix element has to be numerically integrated for the Tassie model, error estimation for the parameters of this model is very time consuming (approximately two orders of magnitude longer than for the generalized Helm model). However, for the first excited state, errors in the Tassie model parameters were evaluated and found to be $c_{\mathrm{tr}} = 2{\cdot}76^{+0{\cdot}98}_{-1{\cdot}66}$ fm, $t_{\mathrm{tr}} = 2{\cdot}16^{+0{\cdot}94}_{-1{\cdot}41}$ fm, $R_{\mathrm{tr}} = 4{\cdot}13 \pm 0{\cdot}12$ fm and $B(\mathrm{E2}, \uparrow) = 275 \pm 20e^2\,\mathrm{fm}^4$. The large errors in c_{tr} and t_{tr} are strongly correlated and merely emphasize the fact that for light nuclei studied in the range of momentum transfer available to the present experiment, the scattering is primarily sensitive to the transition radius rather than the individual parameters of the Fermi distribution.

The slightly larger errors for $B(\mathrm{E2}, \uparrow)$ and R_{tr} as deduced for the Tassie model compared to the generalized Helm model merely reflect the extra variable parameter within the Tassie model framework. However, the statistical errors deduced for the generalized Helm model can be assumed to describe those to be expected for the corresponding Tassie model values.

6. Experimental results

The best-fit parameters and the deduced spectroscopic parameters are given for all the analysed transitions in table 7. It will be noted that the generalized Helm model consistently yields values for $B(\mathrm{E}L, \uparrow)$ and R_{tr} which are of smaller magnitude than the corresponding values deduced from the Tassie model. This point will be discussed in § 7.

The results from the present work will be discussed and compared to previous information for each excited state of ^{26}Mg.

6.1. The ground state

The ground state properties of ^{26}Mg were measured by elastic electron scattering relative to ^{12}C in a separate experiment (Curran *et al* 1972). The data have since been re-analysed using the more accurate ^{12}C ground state parameters reported by Jansen *et al* (1972). A phase-shift analysis of the data employing a two-parameter Fermi distribution yielded for the ground state parameters of ^{26}Mg

$$c = 3{\cdot}04 \pm 0{\cdot}05\ \mathrm{fm}$$

$$t = 2{\cdot}31 \pm 0{\cdot}13\ \mathrm{fm}$$

$$\langle r^2 \rangle^{1/2} = 3{\cdot}06 \pm 0{\cdot}04\ \mathrm{fm}$$

where $\langle r^2 \rangle^{1/2}$ is the RMS radius. These values were used to evaluate the elastic form factor for the inelastic runs.

Table 7. Results for the analysis of the present data using the Tassie model and the generalized Helm model.

		Tassie model				Generalized Helm model				
E_x (MeV)	J^π	c_{tr} (fm)	t_{tr} (fm)	R_{tr} (fm)	$B(iL,\uparrow)$† (e^2 fm^{2L})	β	γ^0	R (fm)	R_{tr} (fm)	$B(iL,\uparrow)$† (e^2 fm^{2L})
1·809	2^+	2·76	2·16	4·13 ± 0·12	275 ± 20	1·937		2·90 ± 0·09	4·04 ± 0·06	266 ± 16
2·945	2^+	1·92	2·61	4·27	7·4	0·346		2·71 ± 0·34	3·90 ± 0·23	6·5 ± 1·4
3·579	0^+					$4·46 \times 10^{-2}$		5·18 ± 0·35	6·17 ± 0·30	17·9 ± 3·9§
4·337	2^+	2·47	2·26	4·08	2·7	0·212		2·75 ± 0·56	3·93 ± 0·39	2·6 ± 1·0
4·875	4^+	1·83	2·31‡	5·59	$3·4 \times 10^4$	1·11		3·47 ± 0·60	4·94 ± 0·42	$(2·6 \pm 0·7) \times 10^4$
4·979	0^+					$3·31 \times 10^{-2}$		5·32 ± 0·31	6·29 ± 0·27	11·1 ± 1·3§
5·294	2^+	1·82	2·20	3·68	3·6	0·404	$0·156^{+0·130}_{-0·156}$	2·13 ± 0·38	3·52 ± 0·23	3·3 ± 0·6
5·449	4^+	2·75‡	2·39‡	5·94‡	$4·6 \times 10^3$	0·248		3·91‡	5·26‡	$3·4 \times 10^3$
5·720	4^+	2·75	2·39	5·94	$1·7 \times 10^4$	0·480		3·91 ± 0·66	5·26 ± 0·49	$(1·3 \pm 0·5) \times 10^4$
6·216	0^+					$2·14 \times 10^{-2}$		5·25‡	6·23‡	$4·4^{+3·1}_{-1·2}$§
6·876	3^-	2·27	2·47	5·07	750	0·677		3·34 ± 0·33	4·62 ± 0·24	638 ± 101
7·082	2^+					0·240	$0·177^{+0·142}_{-0·177}$	2·79 ± 0·30	3·96 ± 0·21	3·5 ± 0·6
7·364	2^+					0·704	0·409 ± 0·081	2·12 ± 0·15	3·52 ± 0·09	10·0 ± 0·6
7·691	3^-	2·27‡	2·47‡	5·07‡	531	0·577		$3·32^{+0·69}_{-1·00}$	$4·60^{+0·50}_{-0·72}$	446 ± 223
7·830	3^-					0·813	0·617 ± 0·200	3·06 ± 0·23	4·42 ± 0·16	546 ± 59
8·181	3^-	3·06	2·31‡	5·11	1050	0·643		3·63 ± 0·26	4·83 ± 0·20	947 ± 154
8·526	2^+					0·195	0·508 ± 0·068	2·13‡	‖	$0·78^{+0·23}_{-0·30}$
8·892	2^+	1·86	2·63	4·27	5·4	0·293		2·74 ± 0·35	3·93 ± 0·24	4·8 ± 1·0
9·287	2^+	2·45	2·31‡	4·13	1·6	0·159		2·79 ± 0·63	3·96 ± 0·44	1·5 ± 0·5
9·860	2^+					$9·82 \times 10^{-2}$	0·293 ± 0·135	3·40 ± 1·59	‖	$1·3^{+1·4}_{-0·9}$
10·199	1^+	3·85	2·40	3·29	$1·14 \times 10^{-2}$	0·619 ± 0·168¶	0·623 ± 0·198¶		3·32 ± 0·20	$(1·3 \pm 0·9) \times 10^{-2}$
10·330	3^-					0·350	$0·264^{+0·315}_{-0·264}$	3·53 ± 0·88	4·76 ± 0·65	238 ± 115
10·491	2^+					0·304	0·258 ± 0·120	$1·98^{+0·92}_{-1·40}$	$3·44^{+0·52}_{-0·79}$	1·4 ± 0·6
10·65	1^+	3·85‡	2·40‡	3·29‡	$1·3 \times 10^{-2}$	0·632¶	0·669¶		3·34	$1·5 \times 10^{-2}$
10·680	4^+	2·75‡	2·39‡	5·94‡	$9·7 \times 10^3$	0·368		3·91‡	$5·26^{+0·82}_{-2·72}$	$(7·4^{+3·7}_{-6·7}) \times 10^3$
10·838	2^+	2·38	2·31‡	4·09	4·5	0·278		2·72 ± 0·62	3·91 ± 0·42	4·3 ± 1·2
10·990	2^+	2·13	2·31‡	3·97	3·7	0·295		2·51 ± 0·50	3·76 ± 0·33	3·4 ± 0·8

† $B(iL,\uparrow)$ (i = E or M) is the ground state reduced transition probability for excitation to the level of spin L.

‡ Denotes that the radius parameter for this level was fixed.

§ The value of the square of the matrix element is quoted for this level in e^2 fm^4.

‖ R_{tr} not evaluated since this level has a strong transverse component.

¶ Values for γ^+ and γ^- for magnetic states are given under the columns β and γ^0 respectively.

6.2. The 1·809 MeV level

The form factor and DWBA fit for this level are shown in figure 4. The present result of $275 \pm 20e^2$ fm^4 for the reduced transition probability differs considerably from the weighted mean of $373 \pm 30e^2$ fm^4 obtained from all other previous measurements.

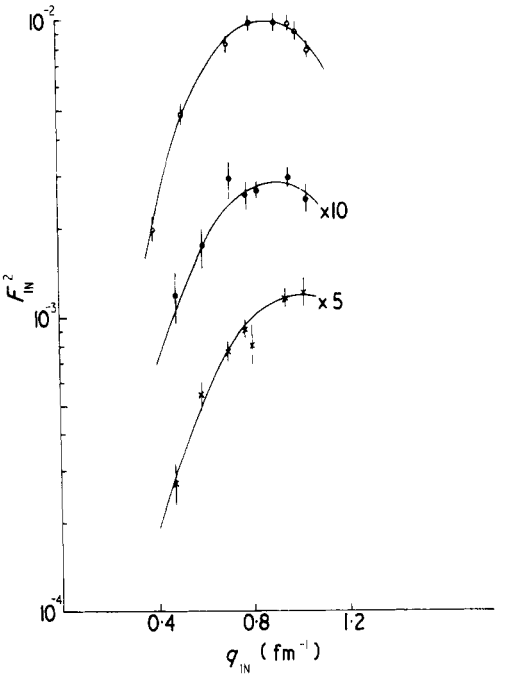

Figure 4. Inelastic form factors for the 2^+ levels in ^{26}Mg at 1·809 MeV (○), 2·938 MeV (●) and 5·294 MeV (×). The full curves are the corresponding best-fit DWBA form factors.

This apparent discrepancy has been discussed fully in a previous publication (Lees *et al* 1973) where it is shown that the present smaller B(E2, ↑) value is more accurate and in closer agreement with theoretical predictions than those values obtained from other experimental techniques. Furthermore, a more detailed study of the individual experimental measurements reveals that the resonance fluorescence, recoil distance and re-orientation experiments yield values for B(E2, ↑) which agree well with the electron scattering result, although the accuracies of these other techniques are poor. In fact, as is shown by Lees *et al* (1973), if the (p, p′γ) DSA experiments are neglected, all results agree within experimental error.

6.3. The 2·938 MeV level

The form factor and DWBA Tassie model fit for this 2^+ level are shown in figure 4. The measured branching ratios for decay to the ground state are 9% (Spilling *et al* 1967), 11 ± 1% (Daniels *et al* 1968), 12 ± 2% (Häusser *et al* 1968), 10% (Pratt 1969), 14% (Selin and Hardnell 1969), $10{\cdot}2 \pm 2$% (Samworth *et al* 1972) and 9 ± 2% (Klotz *et al* 1973). An average branching ratio of 10·7% has been used to extract the reduced transition probabilities listed in table 8. From table 8, it is obvious that the discrepancies in the

Table 8. Details of the DSA lifetime measurements for the 2·938 MeV level of ^{26}Mg.

DSA experiment	Reference	Backing material	Slowing down formalism	τ (fs)	B(E2, ↑) (e^2 fm^4)
(p, p'γ)	a	^{26}Mg	g	50^{+30}_{-20}	40^{+16}_{-24}
(p, p'γ)	b	^{26}Mg O or Ti	h	95 ± 25	21 ± 6
(α, α'γ)	c	^{26}Mg and Au	i	176^{+32}_{-30}	$11{\cdot}3 \pm 2{\cdot}0$
(α, α'γ)	d	^{26}Mg and Au	j	60^{+12}_{-20}	33^{+11}_{-7}
(α, pγ)	e	Ni	h	48 ± 25	42 ± 22
(α, pγ)	f	^{23}Na	h	170 ± 100	12 ± 7

a Häusser *et al* (1968).
b De Kock *et al* (1970).
c Robinson and Bent (1968).
d Haskett and Bent (1972).
e Youngblood *et al* (1967).
f Durell *et al* (1972).
g Lindhard *et al* (1963).
h Lindhard *et al* (1963), Blaugrund (1966).
i Northcliffe (1960), Porat and Ramavataram (1961).
j Extension of Warburton *et al* (1966).

lifetime values obtained from the DSA measurements are even worse than those for the first excited state (Lees *et al* 1973). Broude *et al* (1972) have measured a mean lifetime in ^{22}Ne using 39 backing materials and the electronic and nuclear stopping theory of Lindhard *et al* (1963) as developed by Blaugrund (1966). They report variations of nearly a factor of two in the mean lifetimes measured in different backing materials. In the present situation, not only have different backing materials been used by the various experiments, but different formulations of the stopping theory have been employed (see table 8). It is therefore difficult to draw any definite conclusions regarding the mean lifetime of this level. The weighted mean of the DSA measurements corresponds to a value of $B(\mathrm{E2}, \uparrow) = 14{\cdot}1 \pm 1{\cdot}8 e^2$ fm^4 which is to be compared with the present result of $7{\cdot}4 \pm 1{\cdot}4 e^2$ fm^4.

In the most recent DSA experiment, Durell *et al* (1972) employed the stopping theory of Lindhard and Blaugrund and corrected the measured attenuation factor for feeding from the 3·49 MeV level. The deduced B(E2, ↑) value of $12{\cdot}1 \pm 7{\cdot}1 e^2$ fm^4 is in agreement with the present work.

6.4. The 3·588 MeV level

The 0^+ nature of this state has been well established from triple angular correlation measurements (Broude and Gove 1963) and by ^{24}Mg (t, p) double stripping reactions (Hinds *et al* 1965). The form factor obtained for this transition is shown in figure 5 and there is an obvious difference between the behaviour at high values of momentum transfer of this form factor and those for the C2 transitions at either 1·81 or 2·94 MeV. It is well known that at low values of momentum transfer, the C0 and C2 form factors behave identically and, comparing figures 4 and 5, this is essentially confirmed. However, the peak of the 0^+ form factor occurs at a lower value of momentum transfer, implying a larger transition radius.

The form factor was fitted in PWBA using correction factors generated from the elastic scattering data. The transition radius for this level is $2{\cdot}02 \pm 0{\cdot}10$ times greater than the elastic RMS radius (cf ratio of 1·35 for C2 transitions). This ratio of two for C0 transitions is a common feature in light nuclei (Theissen 1972).

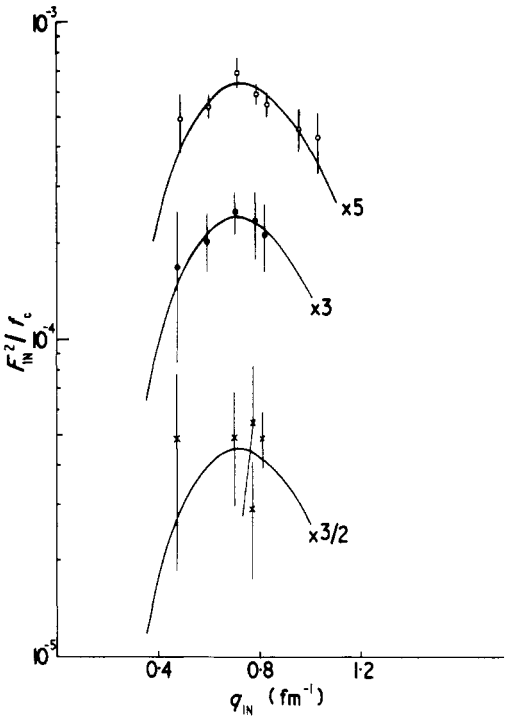

Figure 5. Inelastic form factors for the 0^+ levels in ^{26}Mg at 3·579 MeV (○), 4·979 MeV (●) and 6·216 MeV (×). The full curves are the corresponding best-fit PWBA generalized Helm model form factors. The experimental data points have been corrected for the effects of Coulomb distortion (see § 2).

The matrix element for pair emission is defined (Walecka 1962) as

$$\text{ME} = \langle 0_2^+ | \int r^2 \rho(r)\, \mathrm{d}^3 r | 0_1^+ \rangle$$

and assuming $m_e^2 \ll E_x^2 = \omega^2$

$$\Gamma_0(0_1^+ \to 0_2^+) = \frac{\alpha^2 \omega^5}{135\pi} (\text{ME})^2.$$

For the 3·588 MeV level, the pair emission width is $(8{\cdot}7 \pm 1{\cdot}9) \times 10^{-7}$ eV. No previous measurements of the width exist for comparison.

6.5. *The 3·942 MeV level*

The spin and parity of this level were established as 3^+ by a triple angular correlation study (Ferguson *et al* 1968). M3 transitions in light nuclei are unlikely to be excited in the momentum transfer and angle range ($\theta_{max} = 155°$) at present available at the Kelvin Laboratory. From the raw data, it can be estimated that B(M3, ↑) is unlikely to exceed $2e^2$ fm^6.

6.6. *Triplet of levels at 4·33 MeV*

The energies and spins of the triplet of states at 4·33 MeV are 4·320 MeV, 4^+ (Daniels

et al 1968, Häusser *et al* 1968, Ferguson *et al* 1968, Selin and Hardnell 1969), 4·332 MeV (1, 2^+) (Häusser *et al* 1968, Ferguson *et al* 1968, Klotz *et al* 1973), and 4·350 MeV, 3^+ (Ferguson *et al* 1968). Thus prior to the present experiment the spin and parity of the level at 4·332 MeV were undetermined.

In the present experiment, the form factor for the transition observed at 4·337 ± 0·025 MeV is shown in figure 6. Because of the present experimental resolution, all three levels may be contributing to the measured form factor. The longitudinal–transverse separation of the form factor indicated that no transverse strength was present (ie the transition was not magnetic). Thus, the transition was either a C4 to the 4·320 MeV level and/or a Coulomb transition to the level whose spin and parity were undetermined. The impossibility of fitting the experimental form factor as a C4 transition is clearly demonstrated in figure 6. Therefore only the level at 4·332 MeV was being excited in the present experiment. The data were satisfactorily fitted only by a C2 transition, and thus the spin and parity of the 4·332 MeV level are 2^+.

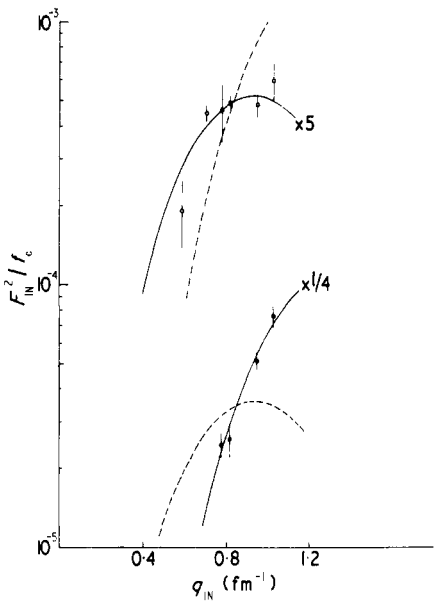

Figure 6. Inelastic form factors for the 2^+ level at 4·337 MeV (○) and the 4^+ level at 4·875 MeV (●). The full curves are the corresponding best-fit PWBA form factors after the experimental data points have been corrected for the effects of Coulomb distortion. The broken curve shown through the 4·337 MeV data points is the best-fit form factor when analysed as an E4 transition. The broken curve shown through the 4·875 MeV data points is the E2 form factor expected for the 4·835 MeV level lifetime measurement of Häusser *et al* (1968).

The branching ratio for decay of the 4·332 MeV level to the ground state has been measured as 5 % (Daniels *et al* 1968), 7 ± 2 % (Häusser *et al* 1968) and less than or equal to 3 % (Selin and Hardnell 1969), 9 ± 3 % (Klotz *et al* 1973). Only two upper limits of the lifetime for this state are available for comparison with the present results, namely, less than 70 fs (Häusser *et al* 1968) and less than 100 fs (Durell *et al* 1972). Using a

branching ratio of $6 \pm 3\%$, the $B(E2, \uparrow)$ values deduced from the lifetime measurements are greater than $2{\cdot}3 \pm 1{\cdot}2$ and greater than $1{\cdot}6 \pm 0{\cdot}8 e^2$ fm^4 respectively both of which agree with the present work.

It might seem surprising that the 4^+ level at 4.32 MeV is not excited in the present experiment, especially since this level is often postulated as being the 4^+ member of the ground state $K = 0^+$ rotational band. However, for the nucleus ^{24}Mg, where the band structure is clearer, the 4^+ member of the ground state band at 4·12 MeV is not excited by inelastic electron scattering (Horikawa *et al* 1971, Johnston and Drake 1974). Further, the extended Nilsson calculations of Drake and Singhal (1971) predict that for both ^{24,26}Mg the $K = 0$, C4 transitions should be weakly excited. Additional E4 transitions were observed at 4·90, 5·45 and 5·72 MeV and the question of the identity of the 4^+ member of the ground state band is discussed in § 8.

6.7. The levels at 4·835 and 4·901 MeV

The 4·835 MeV level has long been established as a 2^+ state. Canada *et al* (1969) have identified the 4·901 MeV level as 4^+ by an angular correlation study. A level was observed in the present experiment at $4{\cdot}875 \pm 0{\cdot}018$ MeV which had the form factor shape characteristic of a C4 transition (see figure 6). Since the measured excitation energy lies outside the accepted value for the 4^+ state, it is possible that some contribution to the form factor from the 4·835 MeV level is present. However, from the raw data it was estimated that $B(E2, \uparrow)$ for the 4·835 MeV level was less than $2e^2$ fm^4.

The data were analysed as a C4 transition using correction factors obtained from the DWBA analysis of the C4 transition at 5·71 MeV. Due to the possible contribution to the form factor from the 4·835 MeV, 2^+ state, the $B(E4, \uparrow)$ value may be overestimated. However, the value of R_{tr} is unlikely to be affected since the 2^+ form factor (see figure 4) has a relatively constant value in the momentum transfer range in which the 4^+ state was observed.

Because of the very small branching ratio of the 4·901 MeV level to the ground state ($\ll 1\%$), it is impossible to compare the present results with the lifetime measurements of Häusser *et al* (1968) and Durell *et al* (1972). For the 4·835 MeV level, the branching ratio to the ground state has been measured as $10 \pm 2\%$ (Daniels *et al* 1968), $13 \pm 2\%$ (Häusser *et al* 1968), 19% (Selin and Hardnell 1969) and $13 \pm 3\%$ (Klotz *et al* 1973). However, Selin and Hardnell (1969) stated that their branching ratios for this level may be subject to a fairly large error and therefore a branching ratio of $12 \pm 2\%$ was adopted. The lifetimes of Häusser *et al* (1968) and Durell *et al* (1972) are less than 50 and less than 90 fs respectively and these correspond to $B(E2, \uparrow)$ values of greater than $3{\cdot}7 \pm 0{\cdot}6$ and greater than $2{\cdot}1 \pm 0{\cdot}4 e^2$ fm^4 respectively. It is possible for the results of Durell *et al* (1972) to be in agreement with the maximum limit of $2e^2$ fm^4 obtained from electron scattering. The $B(E2, \uparrow)$ value as deduced from the lifetime measurement by Häusser *et al* (1968) seems improbable as is demonstrated in figure 6 where a C2 transition for this $B(E2, \uparrow)$ strength is drawn and compared to the experimental data points.

6.8. The 4·972 MeV level

The 0^+ nature of this state was established by ^{24}Mg(t, p) double stripping reactions (Hinds *et al* 1965) and also by triple angular correlation studies (Ferguson *et al* 1968). The equivalent PWBA form factor is shown in figure 5. As for the 3·588 MeV 0^+ level, the

ratio of transition radius for the 4·972 MeV level to the elastic RMS radius is approximately two (2·06 ± 0·09). The ground state width for pair emission is $(2{\cdot}8 \pm 0{\cdot}4) \times 10^{-6}$ eV.

6.9. The 5·291 MeV level

The level at 5·291 MeV has the following possible assignments: 1^+ (Hinds *et al* 1965), 2 (Ferguson *et al* 1968), $(0, 2)^+$ (Blair and Naqib 1970). The form factor measured for this level is shown in figure 4. The longitudinal–transverse separation yielded only a slight transverse strength in excess of the calculated Siegert contribution. Thus the transition cannot be magnetic or C0. The form factor shown in figure 4 has the general shape expected for a C2 transition but appears to reach its maximum at a higher value of momentum transfer than the first excited state, ie implying a smaller transition radius. Similar observations regarding differing form factor shapes for E2 transitions in s–d shell nuclei have been previously reported by Mitsunobu and Torizuka (1972) in ^{20}Ne.

Analysis of the 5·291 MeV level in DWBA using the Tassie model yielded a value for the transition radius which was 11 % smaller than that for the first excited state. Since there are no established values for the spin and parity of this level, the form factor was also fitted as a C3 transition. However, this resulted in a transition radius which was 19 % greater than that for the known C3 transition at 6·88 MeV. Moreover, the minimum χ^2 per degree of freedom increased from 0·7 when fitted as a C2 transition to 2·1 when fitted as a C3 transition. Therefore an assignment of 3^- for this level is most unlikely. Since no other levels are known within 190 keV of the 5·291 MeV level, the experimental form factor cannot be a combination of C2 and C3 transitions measured with poor resolution. Furthermore, two levels at higher excitation energies (7·364 and 10·491 MeV) were discovered which, when analysed as 2^+ levels, had values for R_{tr} similar to that observed for this level. Thus, there would appear to be two types of E2 excitations in this experiment—one group with a ratio of R_{tr} to the elastic RMS radius of approximately 1·35 and the other with a ratio of approximately 1·20. This point will be discussed further in § 8.

The parameter γ^0 was introduced in the generalized Helm model to accommodate the slight transverse contribution present in the form factor. This transverse contribution was not of sufficient strength ($F_e^2/F_C^2 = 1{\cdot}4$ % at 0·77 fm^{-1}) to affect the DWBA Tassie model analysis.

Using the branching ratio for decay to the ground state of 2·5 ± 1·0 % (Häusser *et al* 1968), the B(E2, ↑) values deduced from the lifetime measurements of Häusser *et al* (1968) and Durell *et al* (1972) are greater than 0·5 ± 0·2 and greater than $2{\cdot}5 \pm 1{\cdot}0e^2$ fm^4 respectively. Thus both DSA measurements are in agreement with the present experiment.

6.10. The 5·474 MeV level

Blair and Naqib (1970) established the 4^+ nature of this state by an angular study of inelastic α particle scattering. In the present experiment, this level was weakly excited being observed only at the three highest momentum transfers. A further experimental difficulty occurred in resolving this level on the radiation tail of the strong 2^+ state at 5·294 MeV. As a result, the data obtained on this level were of rather a qualitative nature and it was decided to analyse the form factor by fixing the radius parameters in both models at the values obtained for the C4 transition at 5·72 MeV. It must be emphasized that these results serve only as a guide to the order of magnitude of the transition

strength and are not to be considered as absolute values. However, it can be confidently stated that the transition is not collectively enhanced ($\simeq 1$ Wu).

6.11. The levels at 5·690 and 5·715 MeV

Hinds *et al* (1965) studied these levels by means of stripping and double stripping reactions. They concluded that the 5·715 MeV level was probably a 3^+ and that the excitation of the 5·690 MeV level did not involve a stripping mechanism. From the ^{27}Al(t, α)^{26}Mg reaction, they tentatively assigned a spin of 1 to the 5·690 MeV state. However, this assignment was not based on an angular distribution study but on the assumption that the relative strengths of the levels at $\theta = 50°$ were proportional to $(2J+1)$. As was pointed out by Häusser *et al* (1968), their measured branching ratio of $10 \pm 2\%$ to the ground state for the 5·690 MeV level does not eliminate the possibility that the level may be 2^+. More recently, Blair and Naqib (1970) have suggested that the 5·715 MeV level is a 4^+ state.

The form factor for the level measured at $5{\cdot}720 \pm 0{\cdot}022$ MeV is shown in figure 7 and has the characteristic shape expected for a 4^+ level. The longitudinal–transverse separation of the form factor revealed no magnetic strength and therefore the 3^+ assignment of Hinds *et al* (1965) is incorrect.

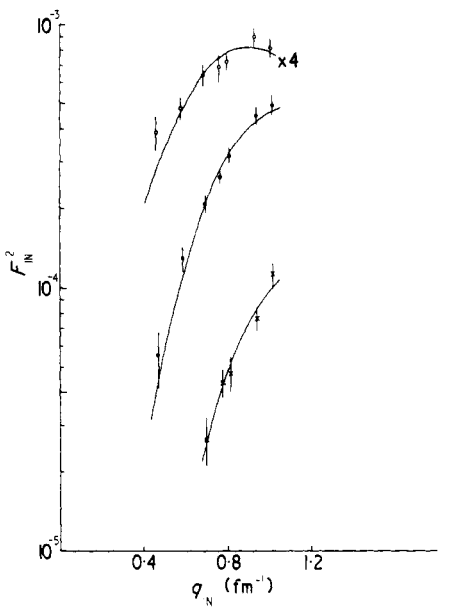

Figure 7. Inelastic form factors for the 2^+ level at 8·892 MeV (○), the 3^- level at 6·876 MeV (●) and the 4^+ level at 5·720 MeV (×). The full curves are the corresponding best-fit DWBA form factors.

In the present experiment, the level at 5·690 MeV was not excited at any value of momentum transfer. From our raw data, it can be concluded that if the 5·690 MeV state is 1^+, then $B(\mathrm{M1}, \uparrow) < 1{\cdot}3 \times 10^{-3} e^2$ fm^2 and if 2^+, $B(\mathrm{E2}, \uparrow) < 0{\cdot}8 e^2$ fm^4. From the lifetime measurements of Häusser *et al* (1968) and Durell *et al* (1972), the following reduced transition probabilities are deduced using a branching ratio of $10 \pm 2\%$ to the

ground state (Häusser *et al* 1968): $B(M1, \uparrow) = 1{\cdot}5 \pm 0{\cdot}9 \times 10^{-5} e^2$ fm^2 and greater than $(2{\cdot}0 \pm 0{\cdot}4) \times 10^{-5} e^2$ fm^2 or $B(E2, \uparrow) = 1{\cdot}0 \pm 0{\cdot}6$ and greater than $1{\cdot}4 \pm 0{\cdot}3 e^2$ fm^4 respectively. It would appear that the 1^+ assignment is more likely but confirmation of the branching ratio result of Häusser *et al* (1968) would be useful.

6.12. The 6 MeV region

Levels have been observed in this region at 6·126 MeV (2^+) (Hinds *et al* 1965, Spilling *et al* 1967, Selin and Hardnell 1969), 6·256 MeV (0^+) (Hinds *et al* 1965, Häusser *et al* 1968), 6·62 MeV (3^+) (Hinds *et al* 1965) and 6·742 MeV $(2, 3)^+$ (Hinds *et al* 1965, Häusser *et al* 1968). This region was weakly excited in the present experiment and, since rescattering effects reached their maximum around this excitation energy, it was difficult to measure these weak transitions.

It was possible to measure the form factor for a level at $6{\cdot}216 \pm 0{\cdot}020$ MeV at only five momentum transfers. These measurements had the general shape of a C0 transition as is shown in figure 5. Because of the deviation of the present excitation energy from the accepted value of 6·255 MeV, it cannot be claimed that the measured form factor is due solely to the excitation of the 0^+ state. However, attempts to fit the measured form factor as a C2 transition required an unusually large transition radius. It would therefore appear that the C0 is the dominant (if not the sole) transition being excited in the present experiment. The form factor was fitted by assuming only a C0 contribution and fixing the radius parameter at the average value of those obtained for the 3·588 and 4·972 MeV C0 transitions. The pair emission width to the ground state is $(3{\cdot}5^{+2{\cdot}5}_{-1{\cdot}0}) \times 10^{-6}$ eV.

6.13. The 6·878 MeV level

The spin and parity of this state were demonstrated by Hinds *et al* (1965) to be 3^-. The present experimental form factor is an excellent example of the characteristic shape of a C3 transition and is shown in figure 7. Comparison of the present $B(E3, \uparrow)$ value and the lifetime of this state (100^{+60}_{-50} fs) as measured by Häusser *et al* (1968), implies a branching ratio for decay to the ground state of $0{\cdot}5 \pm 0{\cdot}3$ %. Spilling *et al* (1967), in their study of γ rays emitted after thermal neutron capture in ^{25}Mg, observed a weak transition of γ-ray energy $6{\cdot}868 \pm 0{\cdot}002$ MeV but the origin of this transition was not identified. However, this transition was not observed by Selin and Hardnell (1969) in a similar experiment.

6.14. The levels at 7·059 and 7·097 MeV

Hinds *et al* (1965) postulated that the level at 7·059 MeV had a spin and parity of 1^- and that the level at 7·097 MeV was a 2^+. Selin and Hardnell (1969) measured the branching ratios of these two states but did not observe any decay to the ground state.

In the present experiment, a form factor was measured for a transition at $7{\cdot}082 \pm 0{\cdot}016$ MeV and is shown in figure 8. The longitudinal–transverse separation of the form factor yielded a transverse strength of 2·2 % at 0·77 fm^{-1} which is in excess of the expected Siegert contribution of 0·32 %. Due to this transverse contribution, only the generalized Helm model was used in the analysis of the form factor. The correction factors used to obtain equivalent PWBA data were derived from the analysis of the 8·89 MeV C2 transition. From figure 8 it is clear that the data are adequately described by an E2 transition.

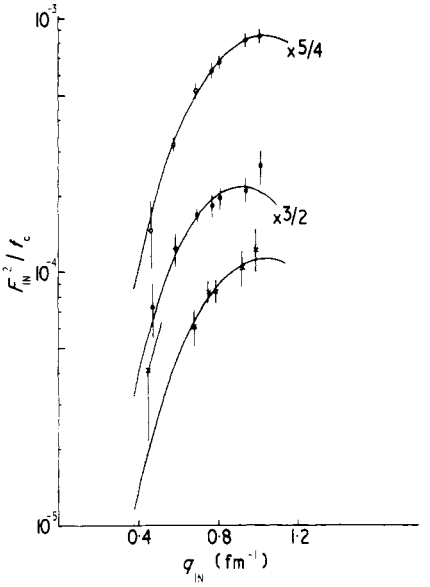

Figure 8. Inelastic form factors for the 2^+ levels in ^{26}Mg at 7·364 MeV (○), 7·082 MeV (●) and 10·491 MeV (×). The full curves are the corresponding best-fit PWBA form factors after the experimental data points have been corrected for the effects of Coulomb distortion.

Thus the dominant and probably the sole transition excited in this region in the present experiment is to the 2^+ level.

6.15. The 7·350 MeV level

No spin–parity assignments have been made in this excitation energy region. The longitudinal–transverse separation of the form factor (figure 3(*a*)) yielded a transverse contribution of 2·25 % at 0·76 fm^{-1} (cf calculated Siegert contribution of 0·35 %) and therefore only the generalized Helm model analysis was applicable. Due to the similarity of the form factor shapes, correction factors derived from the analysis of the 5·29 MeV transition were used and the resulting excellent fit to the data is shown in figure 8. Furthermore, the best-fit radius parameter in the generalized Helm model was identical to that obtained for the 5·29 MeV level. This result is further confirmation of the hypothesis that in the present experiment two types of E2 transition were excited with transition radii differing by 11 %.

Apart from the first excited state, the transition at 7·364 MeV was the strongest E2 observed in our experiment, yet its strength was only 0·43 Wu.

6.16. Doublet at 7·75 MeV

As was discussed in § 4, the doublet of levels was consistently resolved by lineshape analysis. The 7·830 MeV level was found to possess a slight transverse contribution ($\simeq$ 1·7 % at 0·76 fm^{-1}) and accordingly was analysed using only the generalized Helm model. The form factors for the 7·691 and 7·830 MeV levels are shown in figure 9. Correction factors generated from the analysis of the 6·88 MeV level were used for both

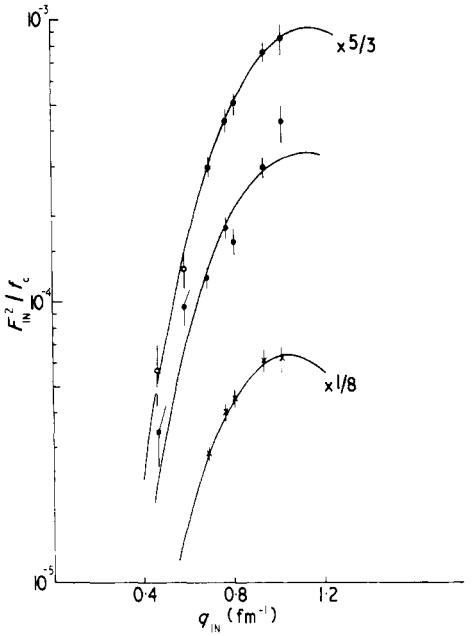

Figure 9. Inelastic form factors for the 3^- levels in ^{26}Mg at 7·830 MeV (○), 7·691 MeV (●) and 8·181 MeV (×). The full curves are the corresponding best-fit PWBA form factors after the experimental data points have been corrected for the effects of Coulomb distortion.

levels. The quality of the E3 fit to the data for the 7·830 MeV level is excellent. The data for the 7·691 MeV level are of a poorer quality and consequently c_{tr} and t_{tr} were fixed in the fitting of the experimental form factor at the values obtained from the analysis of the 6·88 MeV transition. Selin and Hardnell (1969) have observed very weak transitions which they postulated could be decays to the ground state from levels at 7·687 and 7·812 ± 0·004 MeV. The present excitation energies agree very well with their values.

6.17. The 8·181 MeV level

The dependence of the present experimental form factor on momentum transfer was not characteristic of any single multipolarity. However, the shape at higher momentum transfers was characteristic of a C3 transition. This is in contrast with the previous observation of a M1 transition at 8·22 MeV by Titze and Spamer (1966). Furthermore, in the present experiment, the mean excitation energy deduced from the higher momentum transfer spectra was 8·181 ± 0·016 MeV. The present data are consistent with the excitation of an unresolved doublet consisting of a 3^- level at 8·181 MeV and a 1^+ level at 8·22 MeV. Moreover, levels have been observed by Hinds *et al* (1961) at excitation energies of 8·172 ± 0·012 and 8·237 ± 0·010 MeV which are in good agreement with the values measured by electron scattering experiments.

In the present experiment, the longitudinal transition at 8·18 MeV overshadowed the transverse M1 at 8·22 MeV (eg at 0·76 fm^{-1}), the transverse strength was only 2·5% of which 0·4% was due to the Siegert strength for the C3 transition at 8·18 MeV. As a result of this weak M1 contamination of the form factor, the following analysis procedure was adopted. The data points obtained at the lowest momentum transfers and also

those obtained at scattering angles of 140° and 153° were neglected. The C3 fit to the remaining data points is shown in figure 9 and the results are given in table 7. Correction factors from the 6·88 level were used.

Assuming the M1 form factor had the same form factor shape as was obtained for the 10·2 MeV level, the strength of the 8·22 level in the present experiment was estimated to be $B(\mathrm{M1}, \uparrow) \simeq 5 \times 10^{-3} e^2\ \mathrm{fm}^2$. The ratio of peak heights for the 10·2 and 8·22 MeV levels was estimated to be 3·3 from the raw data of Titze and Spamer (1966). Using this ratio and the present experimental result for the strength of the 10·2 MeV level, then $B(\mathrm{M1}, \uparrow) \simeq 4 \times 10^{-3} e^2\ \mathrm{fm}^2$ for the 8·22 MeV level. The encouraging agreement between the two estimates of $B(\mathrm{M1}, \uparrow)$ at different values of momentum transfer implies that the assumption of identical M1 form factor shapes for the 8·22 and 10·20 MeV levels is justified.

Spilling *et al* (1967) measured the branching ratio of a state at $8{\cdot}188 \pm 0{\cdot}001$ MeV to be 100% to the 1·809 MeV level. In contrast, Selin and Hardnell (1969) measured a state at $8{\cdot}185 \pm 0{\cdot}002$ MeV which had branching ratios of 4% to the ground state, 77% to the 1·809 MeV level and 19% to the 2·94 MeV level. Identifying the level measured by Selin and Hardnell (1969) with that studied in the present experiment, if the 4% branching ratio is correct, this implies a mean lifetime of 190 fs which should be accessible to DSA measurements.

6.18. The 8·526 MeV level

In the present experiment, the longitudinal–transverse separation of the form factor for the 8·526 MeV level (see figure 3(*b*)) yielded a transverse strength of 25% at $0{\cdot}76\ \mathrm{fm}^{-1}$. Consequently, only the generalized Helm model was employed in the analysis of the form factor. The fit to the measured form factor as an E2 transition is shown in figure 10.

This E2 assignment is in disagreement with the results of Bendel *et al* (1968) who observed a level at $8{\cdot}52 \pm 0{\cdot}05$ MeV which they analysed as a M1 transition. Their experiment was performed at an electron scattering angle of 180° and as such was only sensitive to the transverse parts of the form factor. However, the present results predict a transverse strength at $0{\cdot}52\ \mathrm{fm}^{-1}$ identical to that observed by Bendel *et al.* At the other momentum transfer studied by them ($0{\cdot}35\ \mathrm{fm}^{-1}$), the extrapolation of the present results yields a value substantially less than their measured cross section. However, their observed cross section at this momentum transfer is very small and the associated error is large and we feel that their data are not inconsistent with the present assignment of a strongly transverse E2 transition. Thus the M1 assignment is doubtful.

Levels were observed in this excitation region by Hinds *et al* (1961) at energies of 8·449, 8·491, 8·521 and 8·566 MeV (all ± 10 keV), indicating that this region may be exceedingly complex to unravel experimentally.

Within the framework of the generalized Helm model, a negative value of R_{tr}^2 was deduced for this level. This negative value may seem surprising but one must remember that it is misleading to interpret the transition radius as physically implying that there is a concentration of the transition charge, current or magnetization densities at the radius $r = R_{\mathrm{tr}}$. This physical interpretation is valid for very simple models and longitudinal transitions, eg liquid drop (Walecka 1962). However, for transverse transitions, no such physical explanation is possible (Drechsel 1968) and R_{tr}^2 can only be considered a convenient parameter for analysing the experiments, especially at low values of momentum transfer. The transition radius for transverse electric transitions is defined

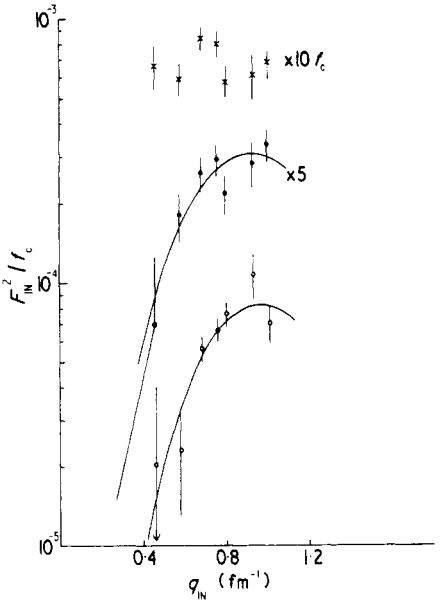

Figure 10. The data points × illustrate the inelastic form factor measured for the transition at 9·287 MeV. The experimental resolution did not permit the separation of the individual contributions from the E2 and M1 transitions. The data points ● represent the E2 transition at 9·287 MeV after the subtraction of the expected form factor contribution from the M1 transition at 9·25 MeV (see text). The data points ○ are for the inelastic form factor for the 2^+ level at 8·526 MeV. All data points for the 8·526 MeV level have been converted to 120° for ease of plotting. The full curves are the corresponding best-fit PWBA form factors after the experimental data points have been corrected for the effects of Coulomb distortion.

(Rosen *et al* 1967) from the relation

$$\left(\frac{B(\mathrm{EL}, q)}{B(\mathrm{EL}, \uparrow)}\right)^{1/2} = 1 - \frac{q^2}{2(2L+3)}\left(\frac{L+3}{L+1}\right)R_{\mathrm{tr}}^2 + \mathrm{O}(q^4).$$

The negative value of R_{tr}^2 arises because in the expansion of the transverse electric form factor at low momentum transfers both the current and magnetization densities contribute to the coefficient of q^2 (equation (2.64*b*), Willey 1963) and the relative phases and magnitudes of the contributions depend critically on the nature of the transition involved.

6.19. The 8·892 MeV level

The form factor for the level measured at 8·892 ± 0·014 MeV is shown in figure 7. Since this level was observed in the low momentum transfer electron scattering experiment of Titze and Spamer (1966) at 8·91 MeV but not in the 180° experiment of Bendel *et al* (1968), the level must be primarily longitudinal. Furthermore, with the limited momentum transfer range available to Titze and Spamer, only transitions of multipolarity 0, 1 and 2 were likely to be excited. In our experiment, the form factor was characteristic of a C2 transition and the longitudinal–transverse separation of the form factor (see figure 3(*a*)) yielded a transverse contribution identical to that expected from the Siegert contribution for a C2 transition. Thus the 2^+ nature of the state is firmly established. In behaviour, the form factor for this transition resembled those for the first and second excited states rather than for the 5·29 MeV level.

Selin and Hardnell (1969) measured the ground state branching ratio for a state at $8{\cdot}904 \pm 0{\cdot}002$ MeV to be 2%. Identifying this state with the one excited in the present experiment implies a mean life of 0·3 fs for this level.

6.20. The doublet at 9·27 MeV

The form factor measured in the present experiment is shown in figure 10. Obviously there are two levels excited in this region which are not resolved by our experiment. One of these has been previously measured by Bendel *et al* (1968) as a 1^+ level at 9·24 $\pm 0{\cdot}03$ MeV. Their data were analysed in PWBA but it has been shown by Chertok and Johnson (1969) that this type of analysis, compared to DWBA, overestimates the $B(\mathrm{M1}, \uparrow)$ and R_{tr} values by 25% and 6·3% respectively for the M1 transition in ^{26}Mg at 10·67 MeV (see § 6.26). Chertok and Johnson also showed that for the 11·42 MeV M1 transition in ^{28}Si, where a similar PWBA analysis was followed, re-analysis in DWBA gave reductions of 27% and 6·25% for $B(\mathrm{M1}, \uparrow)$ and R_{tr} respectively. Assuming that these figures give a reasonable indication of the discrepancy between the results of DWBA and PWBA analysis for all the M1 transitions observed in the experiment of Bendel *et al* (1968), their results for the 9·24 MeV level become $B(\mathrm{M1}, \uparrow) = 9{\cdot}0 \times 10^{-3} e^2$ fm^2 and $R_{\mathrm{tr}} = 3{\cdot}4$ fm. These values were used to subtract the M1 contribution from the form factor measured in the present experiment. The resulting form factor and C2 transition fit are shown in figure 10. Correction factors derived from the analysis of the 8·892 MeV level were used to obtain equivalent PWBA data. Neglecting the lowest momentum transfer runs, the excitation energy of the C2 transition was evaluated as $9{\cdot}287 \pm 0{\cdot}019$ MeV. The earlier electron scattering experiment of Titze and Spamer (1966) also reported a magnetic transition at 9·25 MeV.

Thus, from the three electron scattering experiments it would appear that there are two levels in this region with the following properties: 1^+ at $9{\cdot}25 \pm 0{\cdot}03$ MeV, $B(\mathrm{M1}, \uparrow) = (9{\cdot}0 \pm 2{\cdot}2) \times 10^{-3} e^2$ fm^2 and 2^+ at $9{\cdot}287 \pm 0{\cdot}019$ MeV, $B(\mathrm{E2}, \uparrow) = 1{\cdot}6 \pm 0{\cdot}5 e^2$ fm^4. Other experiments in this region have reported levels at 9·24, 9·31 MeV (Čujec 1964) and $9{\cdot}244 \pm 0{\cdot}012$, $9{\cdot}295 \pm 0{\cdot}012$ MeV (Hinds *et al* 1961). Furthermore, Selin and Hardnell (1969) postulated that a weak transition observed in their ^{25}Mg (n, γ) experiment could be due to the decay of a $9{\cdot}247 \pm 0{\cdot}004$ MeV level to the ground state. Unfortunately, in their experiment the energy of the transition from the capturing state at 11·0935 MeV to the 1·809 MeV level is $9{\cdot}286 \pm 0{\cdot}002$ MeV which probably masked any ground state decay of the 2^+ level observed in the present experiment at $9{\cdot}287 \pm 0{\cdot}019$ MeV.

6.21. The 9·725 MeV level

The level observed at $9{\cdot}725 \pm 0{\cdot}025$ MeV was both very weakly excited and also poorly resolved. No spin and parity assignments can be deduced for this level other than that it may be a doublet involving an M1 transition. The transverse strength is approximately one third of the strength observed at 0·75 fm^{-1}.

6.22. The levels at 9·80 and 9·86 MeV

The experimental form factor is shown in figure 11. In this region of high level density, the combination of the two levels was weakly excited at all values of momentum transfer and consequently the resulting data points are of a poorer standard. The longitudinal–

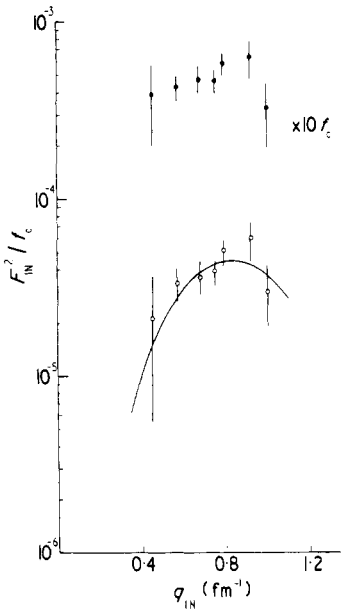

Figure 11. The data points ● represent the experimental form factor for the E2 and M1 transitions at 9·860 and 9·80 MeV respectively. The experimental resolution did not permit the separation of the individual contributions from the two transitions. The data points ○ are for the E2 transition alone after subtracting the M1 contribution to the form factor (see text). All data points have been corrected to 120° for ease of plotting. The full curve is the best-fit PWBA form factor after the experimental data points have been corrected for the effects of Coulomb distortion.

transverse separation of the form factor yielded a 28 % transverse component for this transition at 0·75 fm^{-1} (see figure 3(*b*)).

In the two previous electron scattering experiments, Bendel *et al* (1968) were unable to resolve this region clearly since their experimental resolution appears to have been greater than 200 keV, whilst Titze and Spamer (1966) observed a transverse excitation at 9·80 MeV. Thus, prior to the present work, no strength measurements existed for the levels in this excitation region.

The initial attempt to analyse the data by assuming that the transverse strength measured at 0·75 fm^{-1} was entirely due to a M1 transition resulted in a meaningless residual form factor. However, a combination of a M1 transition and an E2 transition with transverse strength was successfully fitted to the data. The radius parameters and correction factors of the 10·20 MeV level were used for the M1 analysis and correction factors derived from the analysis of the 5·29 MeV level were used for the E2 transition. The fit of the E2 transition to the experimental data after subtracting the M1 contribution is shown in figure 11. Owing to the transverse nature of this E2 transition, the value of R_{tr}^2 deduced within the framework of the Helm model is once again negative (see § 6.18). The strength of the M1 transition was estimated to be about $2{\cdot}4 \times 10^{-3} e^2$ fm^2.

Levels previously observed in this excitation region are 9·814, 9·841 and 9·895 MeV (all ±15 keV) (Hinds *et al* 1961), 9·78, 9·85 and 9·90 MeV (Čujec 1964). Selin and Hardnell (1969) observed an unassigned weak transition of energy 9·858 ± 0·004 MeV.

This may correspond to the ground state decay of the 2^+ level excited in the present experiment.

6.23. The 10·199 MeV level

This level was clearly resolved from the stronger 10·33 MeV (3^-) level only at low values of momentum transfer ($\leqslant 0{\cdot}6\ \text{fm}^{-1}$) or backward angles. The longitudinal–transverse separation of the form factor shown in figure 3(*b*) proved that the level was entirely transverse. The experimental form factor and DWBA fit are shown in figure 12. The results of the present analysis (table 7) agree very well with the values obtained by Bendel *et al* (1968) after allowing for their PWBA analysis (see § 6.20), ie their corrected results are $B(\text{M1}, \uparrow) = (1{\cdot}2 \pm 0{\cdot}3) \times 10^{-2} e^2\ \text{fm}^2$ and $R_{tr} = 3{\cdot}19 \pm 0{\cdot}17$ fm.

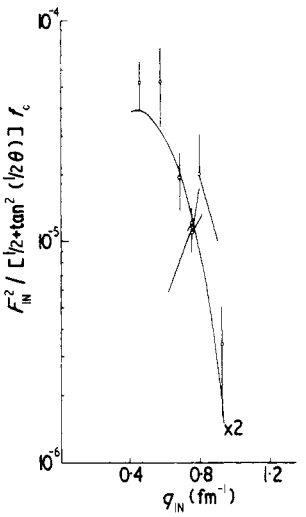

Figure 12. Inelastic form factor for the 1^+ level in ^{26}Mg at 10·199 MeV. The full curve is the best-fit DWBA form factor.

The other electron scattering experiment of Titze and Spamer (1966) observed a transition at 10·20 MeV which was mainly transverse but had a small longitudinal component present. This longitudinal component may have been due to the influence of the 10·33 MeV level which in our momentum transfer range was more strongly excited than the M1 transition at 10·20 MeV.

Kuehne *et al* (1967) in a tagged photon experiment from a natural magnesium target measured a level at $10{\cdot}07 \pm 0{\cdot}05$ MeV which they assigned to be a 1^+ state in ^{26}Mg. There would therefore appear to be a deviation between their measured excitation energy and the values obtained from the three-electron scattering experiment. In the same experiment, Kuehne *et al* also measured the excitation energies for the two strong M1 transitions in ^{24}Mg as $10{\cdot}66 \pm 0{\cdot}02$ and $9{\cdot}92 \pm 0{\cdot}03$ MeV, both of which are lower than the accepted values of 10·737 and 9·984 MeV respectively (Endt and Van der Leun 1967). Thus these results suggest a systematic error of approximately -70 keV in the measurement of excitation energy by Kuehne *et al*. Applying this correction to ^{26}Mg yields an excitation energy of $10{\cdot}14 \pm 0{\cdot}05$ MeV which agrees with the electron

scattering measurements within experimental errors. The result of $\Gamma_0^2/\Gamma = 4{\cdot}2 \pm 0{\cdot}6$ eV obtained by Kuehne *et al* (1967) is compatible with Γ_0 deduced from the electron scattering measurements only if the branching ratio for decay to the ground state is $98 \pm 28\,\%$.

6.24. The 10·33 MeV region

Levels have previously been observed in this excitation region at 10·316 and 10·358 $\pm$0·015 MeV (Hinds *et al* 1961) and 10·31 and 10·35 MeV (Čujec 1964). Thus the transition at $10{\cdot}330 \pm 0{\cdot}020$ MeV observed in the present work is likely to be an unresolved doublet. The longitudinal–transverse separation of the form factor yielded a 4 % transverse contribution which is in excess of the predicted Siegert contribution of either 0·63 % or 0·71 % for a C3 or C2 transition respectively. The form factor shown in figure 13 has a strange behaviour at the lowest value of momentum transfer and implies that the doublet transition may be a combination of a C3 and a lower multipolarity transition.

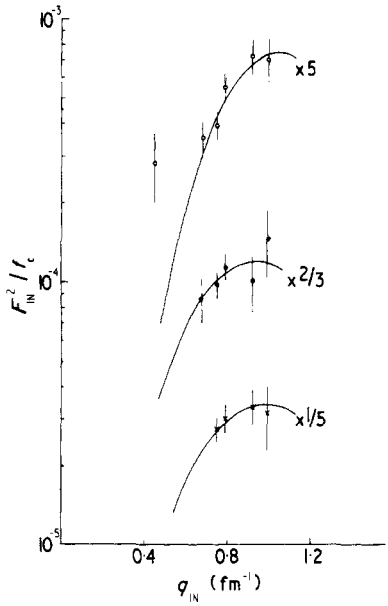

Figure 13. Inelastic form factors for the (3^-) level at 10·330 MeV (○) and the 2^+ levels at 10·838 (●) and 10·990 MeV (×). The full curves are the corresponding best-fit PWBA form factors after the experimental data points have been corrected for the effects of Coulomb distortion.

By assuming that the form factor is resulting solely from the excitation of a 3^- level, the fit shown in figure 13 and the results given in table 7 are obtained by omitting the datum point at 0·45 fm^{-1}. Inclusion of this point changes the $B(E3, \uparrow)$ value by only 16 %. The present 3^- assignment is tentative and accordingly the values for the strength parameters serve as mere indications.

If the data are analysed as arising from the excitation of a 2^+ level, then $B(E2, \uparrow) = 1{\cdot}9 \pm 0{\cdot}9 e^2$ fm^4.

6.25. The 10·491 MeV level

The longitudinal–transverse separation of the form factor yielded a 4·3% transverse strength at 0·75 fm^{-1} (cf calculated Siegert contribution of 0·75%). The equivalent PWBA form factor and generalized Helm model fit are shown in figure 8. The appropriate correction factors were derived from the analysis of the 5·29 MeV level.

It is possible that the level observed at 10·483 ± 0·015 MeV by Hinds *et al* (1961) is the same as that excited in the present experiment.

6.26. The doublet at 10·67 MeV

From the form factor shown in figure 14, it is obvious that two unresolved transitions are being excited in the present experiment. One of these has been reported as a M1 transition at 10·67 MeV (Titze and Spamer 1966) and 10·63 ± 0·03 MeV (Bendel *et al* 1968). From the rapid rise of the present form factor with increasing momentum transfer above 0·8 fm^{-1}, it would appear that the second transition has spin 3 or 4.

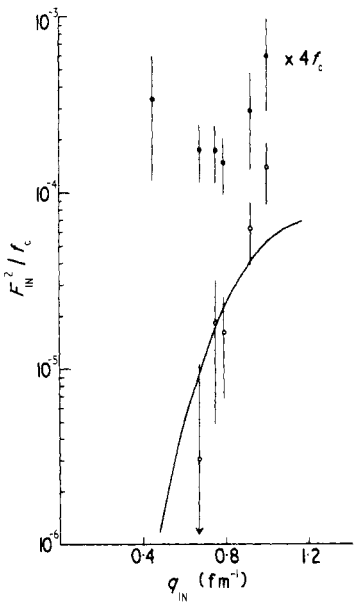

Figure 14. The data points ● represent the experimental form factor for the M1 and E4 transitions at 10·67 MeV which were not resolved by this experiment. The data points ○ are for the E4 transition at 10·680 MeV after subtraction of the M1 contribution to the experimental form factor (see text). The full curve is the best-fit PWBA form factor after the experimental data points have been corrected for the effects of Coulomb distortion.

Further, the longitudinal transverse separation of the form factor shown in figure 3(*a*) indicates a considerable longitudinal strength which cannot be due to magnetic excitations and therefore the second transition must be electric in origin. Thus the most likely combination being excited in this doublet is M1 with either an E3 or E4 transition.

The rapid rise of the form factor at high values of momentum transfer also denotes that it is safe to assume that the form factor measured at 0·45 fm^{-1} is due entirely to the excitation of the 1^+ level. The second level was assumed to have no transverse

strength other than the small contribution expected from the Siegert theorem. This strength was evaluated for both an E3 and an E4 transition and subtracted from the transverse strength measured at 0·75 fm^{-1}. Thus two points on the form factor were obtained which were due to the M1 excitation alone. It was necessary to assume that the values for the radial parameters were identical to those for the 10·20 MeV 1^+ level in order to analyse the M1 transition within the Tassie model framework. The M1 contribution to all the remaining data points was then evaluated and subtracted and the residual form factor analysed as an E3 or E4 transition. The E4 assignment was χ^2-favoured.

The present results obtained for the M1 transition and given in table 7 compare favourably with those deduced by Chertok and Johnson (1969) in their DWBA analysis of the experimental data of Bendel *et al* (1968), namely $B(\mathrm{M1},\uparrow) = 1{\cdot}6 \pm 0{\cdot}6 e^2$ fm^2 and $R_{\mathrm{tr}} = 3{\cdot}25 \pm 0{\cdot}13$ fm.

The magnitude of this 1^+ level affects the value of Γ_0^2/Γ obtained by Kuehne *et al* (1967) for the 10·74 MeV level in ^{24}Mg, since they used a natural magnesium target and their experimental resolution did not enable them to resolve the 10·65 MeV ^{26}Mg level from the 10·74 MeV ^{24}Mg level. The level width from the ground state Γ_0 for the 10·74 MeV level is 12·7 eV (Johnston and Drake 1974) whilst that for the 10·65 MeV level is 6 eV (Chertok and Johnson 1969, present work). Although the isotopic abundance ratio is 7·06 in favour of ^{24}Mg, the influence of the ^{26}Mg level on the measurements of Kuehne *et al* depends critically on the branching ratio to the ground state for both levels. For ^{24}Mg, this branching ratio has been measured as 40% (Lawergren *et al* 1970). Assuming a ground state branching ratio of 100% for the 10·65 MeV ^{26}Mg level, then the Γ_0^2/Γ value of Kuehne *et al* should be reduced by 17%. This reduction is correspondingly less if the ^{26}Mg branching ratio is lower.

6.27. The levels at 10·838 and 10·990 MeV

These levels were not measured in all experimental runs. The form factors for these levels are shown in figure 13. Both had the general shape of E2 transitions and were analysed using correction factors derived from the analysis of the 8·89 MeV level.

The level at $10{\cdot}838 \pm 0{\cdot}024$ MeV has not been previously observed. As regards the other level, Čujec (1964), studying ^{25}Mg(d, p)^{26}Mg reactions has observed two levels at excitation energies of 10·98 and 11·00 MeV but no spin–parity assignments were made.

For convenience, table 9 lists the results of the present experiment for those levels of excitation energy greater than 8 MeV and compares these results with those of the two previous electron scattering measurements.

7. Model dependence

The errors in the reduced transition probabilities and transition radii quoted above are purely statistical. This section discusses the extent to which the deduced spectroscopic parameters are subject to a systematic error arising from the assumption of a particular nuclear model in the data analysis. This 'model-dependence' error has been fully discussed by Singhal *et al* (1974). They showed that, by comparing electron scattering results analysed with the Tassie model for ^{60}Ni and ^{90}Zr with accurate model independent measurements of B(E2, ↑) (eg (γ, γ') and Coulomb excitation), this error is less than

Table 9. Comparison of the results obtained by the inelastic electron experiments for ^{26}Mg in the excitation energy region from 8 to 11 MeV.

Present experiment				Titze		Bendel		
E_x (MeV)	J^π	$B(iL,\uparrow)$ (e^2fm^{2L})	R_{tr} (fm)	E_x (MeV)	Type†	E_x (MeV)	$B(M1,\uparrow)$ ($10^{-2}e^2$fm^2)	R_{tr} (fm)
8·181	3^-	1050	5·11	—	—	—	—	—
—	1^+	$\simeq 5\times10^{-3}$	3·29	8·22	t	—	—	—
8·526	(2^+)	0·78	‡	8·57	t	8·52	0·17	3·0
8·892	2^+	5·4	4·27	8·91	l	—	—	—
—	1^+	—	—	9·25	t	9·24	0·90	3·4
9·287	2^+	1·6	4·13	—	—	—	—	—
9·727	—	—	—	9·58	—	9·67	0·40	2·7
—	1^+	$\simeq 2{\cdot}4\times10^{-3}$	3·29	9·80	t	—	—	—
9·860	2^+	1·3	‡	—	—	—	—	—
10·199	1^+	$1{\cdot}2\times10^{-2}$	3·29	10·20	t	10·18	1·16	3·2
10·330	3^-	238	4·76	—	—	—	—	—
10·491	2^+	1·4	3·44	—	—	—	—	—
10·65	1^+	$1{\cdot}4\times10^{-2}$	3·34	10·67	t	10·63	1·62	3·25
10·680	4^+	$9{\cdot}7\times10^{3}$	5·94	—	—	—	—	—
10·838	2^+	4·5	4·09	—	—	—	—	—
10·990	2^+	3·7	3·97	—	—	—	—	—

† t = transverse excitation, l = longitudinal excitation.

‡ R_{tr} not evaluated since transition has large transverse electric component.

5 % for E2 transitions provided the data spans the momentum transfer range given by $1{\cdot}5 \leqslant qR_{tr} \leqslant 6{\cdot}0$. For the limited range $1{\cdot}65 \leqslant qR_{tr} \leqslant 4{\cdot}3$ used in the present experiment, some model dependence may exist. It is not possible to deduce this by comparison with accurate model-independent measurements since none exist for ^{26}Mg (Lees *et al* 1973). However, for limited momentum transfer ranges similar to that used in the present experiment, Metzger (1970) and Johnston (1972) have shown that for a Tassie model analysis the model dependence of electron scattering is less than 10 %. This value is smaller than the quoted statistical uncertainty for most of the transitions measured in the present experiment.

Another useful indication of the extent to which any model dependence may be present can be obtained by comparing the results from the two phenomenological models used in the data analysis. It has already been mentioned in § 6 that the generalized Helm model consistently yields slightly smaller values for $B(EL,\uparrow)$ and R_{tr} than the Tassie model. These differences are illustrated graphically as a function of multipolarity in figure 15 for electric transitions. The differences between the two models are empirically found to increase with the square of the multipolarity for both $B(EL,\uparrow)$ and R_{tr} but the increase is more pronounced for $B(EL,\uparrow)$. The large difference in $B(E4,\uparrow)$ values probably simply reflects the fact that the range of qR_{tr} is more restricted ($4{\cdot}16 \leqslant qR_{tr} \leqslant 6{\cdot}07$) for E4 transitions than for the lower multipolarities.

The statistical errors associated with the magnetic transitions considerably exceed the observed differences between the two phenomenological models. However, the agreement between the present results and the model-independent electron scattering results at low energies (Bendel *et al* 1968) appears to indicate that any such model dependence for M1 transitions is small.

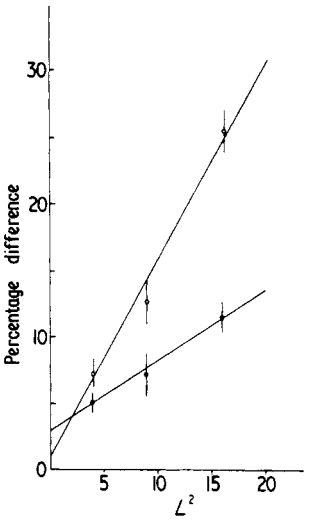

Figure 15. The average differences between the Tassie model and the generalized Helm model results are plotted against the square of the multipolarity of the transition. The data points ○ are for the electric reduced transition probabilities, $B(EL, \uparrow)$, and those ● are for the transition radii R_{tr}. The full curves are the corresponding best-fit straight lines.

Thus the comparison of the two phenomenological models lends support to the belief that, for low multipolarity transitions, the model dependence is likely to be less than 10% which is usually less than the present statistical accuracy. For the higher multipolarity transitions, the model dependence is likely to increase but again is usually less than the present statistical accuracy.

8. Theoretical comparison

8.1. Level scheme

The theoretical spectra for the positive parity states of ^{26}Mg below 6·25 MeV are illustrated in figure 16. The experimental spins are derived from the previous and present work discussed in § 6. From figure 16, it is clear that the only model which accounts for all the known positive parity levels below 6 MeV is that of a rotor core with two interacting valence neutrons (Craig 1973). This model was formulated in the strong-coupling limit using an axially symmetric ^{24}Mg core. The present work in identifying the 2^+ nature of the states at 4·33 and 5·29 MeV is in agreement with the prediction of this model. Furthermore, the model predicts the assignment of 1^+ to the 5·69 MeV state which is also the more likely value deduced from the measurements of Häusser *et al* (1968) and the present work. The major discrepancy between Craig's prediction and the experimental spectrum is the failure to reproduce the experimental 2, 0, 3 spin sequence at 2·94, 3·58 and 3·94 MeV respectively.

The situation regarding the identity of the 4^+ member of the ground state band is confusing. Calculations prior to Craig (1973) usually associated the 4^+ level at 4·33 MeV as belonging to the ground state rotational band. However, the measured ratio of $R = B(E2, 4^+ \rightarrow 2^+)/B(E2, 2^+ \rightarrow 0^+) = 0{\cdot}39 \pm 0{\cdot}14$ deduced from the lifetime measurements of Durell *et al* (1972) and Häusser *et al* (1968) is in poor agreement with the value

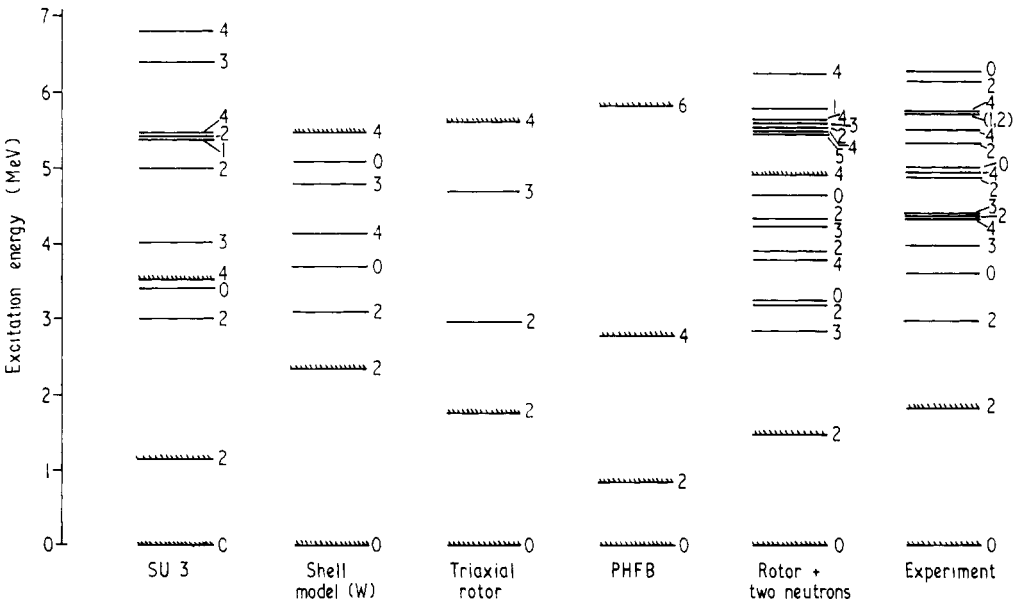

Figure 16. The experimental positive-parity states of ^{26}Mg below 6·5 MeV compared to the various theoretical predictions. The levels indicated by hatching are to be identified as members of the $K = 0$, ground state rotational band. The references are SU3 (Stewart and Castel 1969), shell model (W) (Bell *et al* 1969), triaxial rotor (Kurath 1972), PHFB (Goeke *et al* 1973) and rotor plus two neutrons (Craig 1973).

of 1·43 expected for an unmixed $K = 0$ rotational band. This fact led Durell *et al* (1972) to propose that ^{26}Mg may be analogous to ^{30}Si where the collective 4^+ strength is shared between two or more levels. The present work has revealed possible candidates for sharing this strength at 4·90, 5·45 and 5·72 MeV. However, Craig (1973) obtained solutions which indicated that the ground state band for ^{26}Mg was remarkably pure $K = 0$, ie 99·6% for the 2^+ member with decreasing purity to 77% for the 8^+ member. In addition, his wavefunction for the collective 4^+ state was not very sensitive to the choice of the residual interaction employed. On the basis of these two observations, he concluded that sharing of the collective 4^+ strength was unlikely. Nevertheless, his identification of the second 4^+ level at 4·90 MeV as belonging to the ground state band is still not satisfactory from an experimental point of view. Assuming that the 4·90 level belongs to the ground state band, the value of R can be deduced from the lifetime measurements of Häusser *et al* (1968) and Durell *et al* (1972) to be $0{\cdot}61 \pm 0{\cdot}22$ which is still in poor agreement with that expected for an unmixed band. However, it is possible that evaluation of the theoretical electromagnetic transition rates and electron scattering form factors will clarify the problem.

8.2. Transition probabilities and quadrupole moment

Within the framework of the axially symmetric rotational model, the present $B(E2, \uparrow)$ value for the first excited state yields a magnitude of 53 fm^2 for the intrinsic quadrupole moment Q_0. By the re-orientation effect, Schwalm *et al* (1972) have measured ^{26}Mg to be prolate and list values of Q_0 as 56 ± 14 or 42 ± 14 fm^2. The two possible magnitudes

arise from the uncertainty of the sign of the interference term for virtual excitations through the second excited 2^+ state. The larger value is in good agreement with the present work and is compared to the various theoretical predictions listed in table 10.

Table 10. Comparison of the experimental value for the intrinsic quadrupole moment with the various theoretical predictions.

Description	$Q_0(\text{fm}^2)$	Reference
$1d\frac{5}{2}$–$2s\frac{1}{2}$ shell model ($\epsilon = 0{\cdot}7$)	$-1{\cdot}4$	Wildenthal *et al* (1971)
HF—first 5 shells ($\epsilon = 0{\cdot}2$)	$+63{\cdot}4$	Gunye (1971)
Nilsson—first 7 shells	$+66{\cdot}8$	Drake and Singhal (1971)
Triaxially deformed rotor (s–d shell) ($\epsilon = 0{\cdot}5$)	$+45{\cdot}5$	Kurath (1972)
HFB—first 3 shells	$+34{\cdot}7$	Goeke *et al* (1973)
Experimental result	$+56\pm14$	Schwalm *et al* (1972)

Only the severely truncated shell model calculation of Wildenthal *et al* (1971) is in violent disagreement with the experimental result. The projected Hartree–Fock–Bogoliubov (HFB) calculation of Goeke *et al* (1973) and the triaxially deformed rotor of Kurath (1972) illustrate the findings of Lee and Cusson (1972), namely, the inclusion of higher shells is essential before the electromagnetic properties of s–d shell nuclei can be reproduced.

It is interesting to compare the HF calculations of Gunye (1971) with the HFB calculation of Goeke *et al* (1973). This comparison is reasonably valid since Goeke *et al* (1973) also performed HF calculations for ^{26}Mg and found that pairing had little effect on the intrinsic properties. After eliminating the effective charge of $0{\cdot}2e$ from the result of Gunye (1971), comparison of the two calculations shows that the inclusion of the 2plf and 3s2dlg shells increases Q_0 from 34·7 to 44·2 fm^2. This 27% increase is of similar magnitude to that observed by Gunye for other even–even s–d shell nuclei. The two HF solutions can be made to agree very well with the experimental result by the use of effective charges of $0{\cdot}1e$ for the HF and $0{\cdot}3e$ for the HFB calculations.

The comparison of the present transition probability for the first excited state with various theoretical predictions has already been published (Lees *et al* 1973). Table 11 lists the predicted transition probabilities from the ground state to the lower-lying

Table 11. Comparison of the present results for the reduced transition probabilities with the various theoretical predictions.

Reduced transition probabilities (e^2 fm^{2L})			
$0_1^+ \rightarrow 2_1^+$	$0_1^+ \rightarrow 2_2^+$	$0_1^+ \rightarrow 3_1^+$	Reference
190	4·0	0·2	W } Bell *et al* (1969)
199	17·6	4·4	K } Bell *et al* (1969)
340	0	—	Wildenthal *et al* (1972)†
280	5	—	Kurath (1972)
275 ± 20	$7{\cdot}4\pm1{\cdot}6$	<2	Present work

† Private communication in Kurath (1972).

levels and compares them to the present experimental results. The calculations of Bell *et al* (1969) employed both the two-body matrix elements and single-particle energies which had been obtained empirically by Wildenthal *et al* (1968) and also the reaction matrix elements of Kuo (1967) corrected for interactions with the ^{16}O core. These are labelled W and K respectively in table 11. Both calculations of Bell *et al* (1969) and also that of Wildenthal *et al* (1972, private communication in Kurath 1972) restricted the active orbitals to the $1d\frac{5}{2}$ and $2s\frac{1}{2}$ shells. Not surprisingly, the results of Kurath (1972) using the entire 2s–1d shell are in better agreement with the present experiment.

8.3. Form factor comparison

The form factors obtained from inelastic electron scattering experiments can be used as a critical test for nuclear models. For example, several nuclear models may yield the same reduced transition probability yet differ substantially in the radial dependence of the transition matrix element. This difference will be revealed in the predicted form factors of the various nuclear models especially at large values of momentum transfer. It is therefore unfortunate that, apart from the Nilsson model prediction for the 1·81 MeV level (Drake and Singhal 1971), no detailed theoretical form factors are available for comparison with the present work. This Nilsson model comparison has been discussed elsewhere (Lees *et al* 1973).

In an attempt to illustrate the power of the electron scattering technique in a simple fashion, independent-particle shell model (IPSM) calculations were performed for the C2 and M1 transitions observed in the present experiment. The angular momentum and radial matrix elements used are given by Willey (1963). The form factors were corrected for finite proton size and for centre of mass motion following Elton (1961).

8.3.1. M1 transitions. The HFB calculations of Morrison (1973, private communication) indicate that although the ground state of ^{26}Mg was predominantly $1d\frac{5}{2}$, a considerable $2s\frac{1}{2}$ wavefunction was present. Thus IPSM calculations were performed for the possible transitions $1d\frac{5}{2}$ to $1d\frac{3}{2}$ and also $2s\frac{1}{2}$ to $1d\frac{3}{2}$ and compared to the experimental form factor for the 10·2 MeV transition. This transition was typical of all the M1 transitions excited in the present experiment. The results are illustrated in figure 17 from which it is obvious that the $2s\frac{1}{2}$ to $1d\frac{3}{2}$ transition has completely the wrong momentum transfer dependence to account for any of the M1 transitions excited in the present experiment. For the $1d\frac{5}{2}$ to $1d\frac{3}{2}$ transition it was necessary to use an oscillator parameter of 1·95 fm to reproduce the exact momentum transfer dependence of the experimental form factor.

8.3.2. C2 transitions. One of the most interesting facets of this experiment was the discovery that the C2 transitions of single-particle strength appeared to lie in one of two distinct groups of transition radius. That these two groups had differing excitation strengths as a function of momentum transfer is clearly indicated in figure 18. This figure shows the ratio of the experimental form factors for the 2^+ levels at 7·36 MeV ($R_{tr} = 3{\cdot}52 \pm 0{\cdot}09$ fm) and 2·94 MeV ($R_{tr} = 3{\cdot}90 \pm 0{\cdot}23$ fm). The ratio increases with the value of momentum transfer reflecting the smaller transition radius of the 7·36 MeV level. A form factor ratio of identical slope to that illustrated in figure 18 is obtained if the 5·29 MeV level is plotted relative to the 2·94 MeV level. Also shown in figure 18 is the form factor ratio for the known 3^- level at 6·88 MeV with respect to the 7·36 MeV

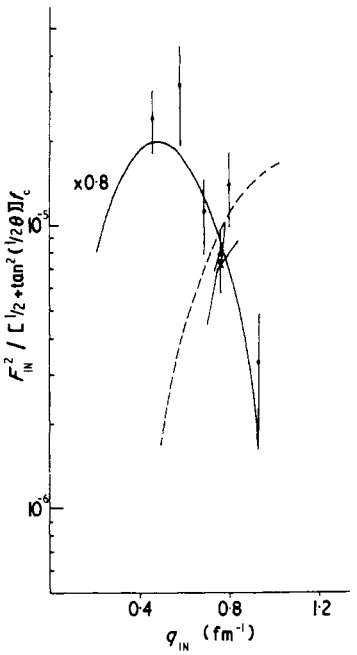

Figure 17. The IPSM predictions in PWBA for the M1 form factor of the 10·199 MeV level in ^{26}Mg. The full curve is for a single-particle transition from the $1d\frac{5}{2}$ to $1d\frac{3}{2}$ orbitals for an oscillator parameter of 1·95 fm. An overall normalization of 0·8 was required to fit the experimental data. The broken curve is for a transition from the $2s\frac{1}{2}$ to $1d\frac{3}{2}$ orbitals. The experimental data points have been corrected for the effects of Coulomb distortion.

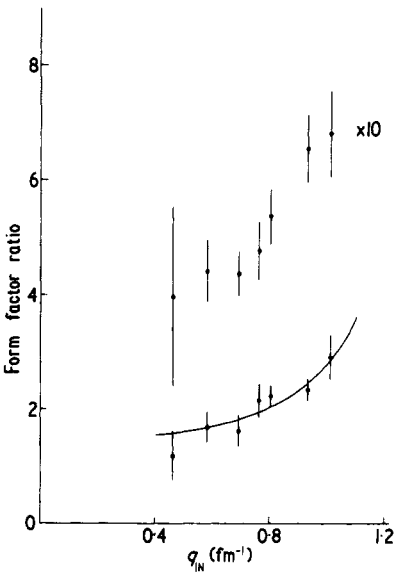

Figure 18. Form factor ratios for the 6·876 MeV, E3 and 7·364 MeV, E2 transitions (○) and for the E2 transitions at 7·364 and 2·945 MeV (●) as a function of momentum transfer. The full curve is the IPSM ratio expected for the $d\frac{5}{2}$ to $d\frac{3}{2}$ transition compared to the $d\frac{5}{2}$ to $s\frac{1}{2}$ transition (see text).

level. This latter ratio increases rapidly with increasing momentum transfer and thus provides further evidence that the levels at 5·29 and 7·36 MeV have spin and parity 2^+ although their momentum transfer dependence is intermediate between that of a normal C2 and C3 transition.

Differing form factor shapes for C2 transitions have been previously noted for the 7·43 and 7·84 MeV transitions in ^{20}Ne (Mitsunobu and Torizuka 1972) but no explanation was offered. In an attempt to understand in a simple fashion why there should be two distinct values of R_{tr}, the Coulomb form factors for transitions of multipolarity 2 were evaluated using the IPSM. There are three possible subshell transitions within the 2s–1d shell: $1d\frac{5}{2}$ to $2s\frac{1}{2}$, $1d\frac{5}{2}$ to $1d\frac{3}{2}$ and $2s\frac{1}{2}$ to $1d\frac{3}{2}$. Within the framework of this model, the $1d\frac{5}{2}$ to $2s\frac{1}{2}$ and $2s\frac{1}{2}$ to $1d\frac{3}{2}$ transitions have the same dependence on momentum transfer. Thus the ratios of the predicted form factors for the $1d\frac{5}{2}$ to $1d\frac{3}{2}$ and the $1d\frac{5}{2}$ to $2s\frac{1}{2}$ transitions were evaluated as a function of momentum transfer. The oscillator parameter was arbitrarily fixed at the value obtained from the IPSM fit to the M1 transition (ie 1·95 fm). The resulting shape reproduces the experimental ratios very closely as is shown in figure 18.

The agreement of the IPSM predictions with the experimental form factors for both the M1 and C2 transitions is encouraging using such a simple approach. Although the oscillator parameter used is 12% in excess of the value expected from the $A^{1/3}$ rule, deviations twice as large are by no means uncommon for IPSM form factor calculations (De Forest and Walecka 1966).

9. Conclusions

The present work has extended the spin and parity assignments in ^{26}Mg up to an excitation energy of 11 MeV. The ground state reduced transition probabilities and transition radii were also measured. On comparing the reduced transition probabilities with those deduced from other work, it was found that the present work yielded more precise values. Difficulties were encountered in resolving the dense but weakly excited region between 8·5 and 11 MeV and perhaps the higher resolution electron scattering facilities currently under construction will resolve the remaining uncertainties in this region.

The present results have been compared with the limited number of theoretical predictions available. The calculation of Craig (1973) assuming a rotor core and two interacting valence neutrons reproduces the low-lying level scheme very well. It is unfortunate that no transition probabilities were evaluated by Craig, since the reproduction of experimental transition rates is a superior test of any nuclear model. Most of the existing calculations for transition probabilities are severely truncated in size and hence are not able to reproduce the electromagnetic properties of ^{26}Mg. However, using the simple ideas of the IPSM it was shown that the M1 transitions observed in the present experiment can be understood in terms of a simple $1d\frac{5}{2}$ to $1d\frac{3}{2}$ transition and also that two C2 transitions with differing dependence on momentum transfer may be expected from the differing behaviour of the $1d\frac{5}{2}$ to $1d\frac{3}{2}$ and $1d\frac{5}{2}$ to $2s\frac{1}{2}$ transitions.

Acknowledgments

The authors would like to thank the UK Science Research Council for grants supporting

this work. One of the authors (CSC) is grateful to the Carnegie Trust for financial support. The authors also acknowledge the interest and encouragement expressed by Professor G R Bishop.

References

Bell R A I *et al* 1969 *Nucl. Phys.* A **133** 337–56
Bendel W L *et al* 1968 *Phys. Rev.* **173** 1103–7
Bergstrom J C *et al* 1971 *Phys. Rev.* C **4** 1514–32
Blair J S and Naqib J M 1970 *Washington University, Seattle* Preprint
Blaugrund A E 1966 *Nucl. Phys.* **88** 501–12
Broude C and Gove H E 1963 *Ann. Phys., NY* **23** 71–122
Broude C *et al* 1972 *Phys. Lett.* **39B** 185–7
Canada T R, Bent R D and Haskett J A 1969 *Phys. Rev.* **187** 1369–77
Chertok B T and Johnston W T K 1969 *Phys. Rev. Lett.* **22** 67–70, 265
Cline D and Lesser P M S 1970 *Nucl. Instrum. Meth.* **82** 291–3
Craig G 1973 *Technische Hochschule Darmstadt* Preprint IKDA 73/11
Čujec B 1964 *Phys. Rev.* **136** B1305–24
Curran C S *et al* 1972 *J. Phys.* A: *Gen. Phys.* **5** L39–42
Daniels T *et al* 1968 *Nucl. Phys.* A **110** 339–52
De Forest T and Walecka J D 1966 *Adv. Phys.* **15** 1–109
De Kock P R *et al* 1970 *Nucl. Phys.* A **140** 190–200
Drake T E and Singhal R P 1971 *Glasgow University Internal Report*
Drechsel D 1968 *Nucl. Phys.* A **113** 665–75
Duguay M A *et al* 1967 *Phys. Rev.* **163** 1259–77
Durell J L *et al* 1972 *J. Phys.* A: *Gen. Phys.* **5** 302–17
Elton L R B 1961 *Nuclear Sizes* (London: Oxford University Press) pp 21–2
Endt P M and Van der Leun C 1967 *Nucl. Phys.* A **105** 1–488
Ferguson A J *et al* 1968 *Bull. Am. Phys. Soc.* **13** 86
Goeke K *et al* 1973 *Nucl. Phys.* A **208** 477–502
Gunye M R 1971 *Phys. Lett.* **37B** 125–7
Haskett J A and Bent R D 1971 *Phys. Rev.* C **4** 461–70
Häusser O, Alexander T K and Broude C 1968 *Can. J. Phys.* **46** 1035–50
Hinds S, Marchant H and Middleton R 1961 *Proc. Phys. Soc.* **78** 473–90
—— 1965 *Nucl. Phys.* **67** 257–70
Hogg G R *et al* 1972 *Nucl. Instrum. Meth.* **101** 203–19
Horikawa Y *et al* 1971 *Phys. Lett.* **36B** 9–11
Isabelle D B and Bishop G R 1963 *Nucl. Phys.* **45** 209–34
Jansen J A *et al* 1972 *Nucl. Phys.* A **188** 337–52
Johnston A 1972 *PhD Thesis* University of Glasgow
Johnston A and Drake T E 1974 *J. Phys.* A: *Math., Nucl. Gen.* **7** 898–935
Khvastunov V M *et al* 1970 *Sov. J. nucl. Phys.* **12** 5–8
Klotz G *et al* 1973 *Nucl. Phys.* A **205** 90–6
Kuehne H W, Axel P and Sutton D C 1967 *Phys. Rev.* **163** 1278–91
Kuo T T S 1967 *Nucl. Phys.* A **103** 71–96
Kurath D 1972 *Phys. Rev.* C **5** 768–72
Lawergren B *et al* 1970 *Phys. Rev.* C **1** 994–9
Lee H C and Cusson R Y 1972 *Ann. Phys., NY* **72** 353–427
Lees E W 1972 *PhD Thesis* University of Glasgow
Lees E W *et al* 1973 *J. Phys.* A: *Math., Nucl. Gen.* **6** L116–20
Lindhard J *et al* 1963 *K. danske Vidensk Selsk., Math.-fys. Meddr* **33** No 14
Maximon L C 1969 *Rev. mod. Phys.* **41** 193–204
Metzger F R 1970 *Nucl. Phys.* A **148** 362–8
Mitsunobu S and Torizuka Y 1972 *Phys. Rev. Lett.* **28** 920–2
Northcliffe L C 1960 *Phys. Rev.* **120** 1744–57
Porat D I and Ramavataram K 1961 *Proc. Phys. Soc.* **78** 1135–43

Powell M J D 1971 *AERE Library Subroutine, Harwell* R6912, 72–3
Pratt T A E C 1969 *Nuovo Cim.* B **61** 119–30
Rawitscher G H and Fischer C R 1961 *Phys. Rev.* **122** 1330–7
Robinson S W and Bent R D 1968 *Phys. Rev.* **168** 1266–86
Rosen M, Raphael R and Uberall H 1967 *Phys. Rev.* **163** 927–34
Samworth E A *et al* 1972 *Phys. Rev.* C **5** 138–42
Schucan T H 1968 *Phys. Rev.* **171** 1142–50
Schwalm D *et al* 1972 *Nucl. Phys.* A **192** 449–95
Selin E and Hardnell R 1969 *Nucl. Phys.* A **139** 375–84
Singhal R P *et al* 1974 *Nucl. Phys.* A **218** 189–200
Spilling P *et al* 1967 *Nucl. Phys.* A **102** 209–25
Stewart K W C and Castel B 1969 *Nucl. Phys.* A **132** 445–54
Tassie L J 1956 *Aust. J. Phys.* **9** 407–18
Theissen H 1972 *Springer Tracts in Modern Physics* vol 65 (Berlin: Springer-Verlag) pp 1–57
Titze O and Spamer E 1966 *Z. Naturf.* **21a** 1504–6
Tuan S T *et al* 1968 *Nucl. Instrum. Meth.* **60** 70–6
Walecka J D 1962 *Phys. Rev.* **126** 653–62
Warburton E K *et al* 1966 *Phys. Rev.* **148** 1072–82
Wildenthal B H *et al* 1968 *Phys. Lett.* **26B** 692–4
Wildenthal B H *et al* 1971 *Phys. Rev. Lett.* **26** 96–9
Willey R S 1963 *Nucl. Phys.* **40** 529–65
Youngblood D H *et al* 1967 *Phys. Rev.* **164** 1370–4